Development of hydro-meteorological drought index under climate change – Semi-arid river basin of Peninsular India

by

Shaik Rehana, G. Sireesha Naidu

in

Journal of Hydrology

Report No: IIIT/TR/2021/-1

Centre for Spatial Informatics
International Institute of Information Technology
Hyderabad - 500 032, INDIA
January 2021

Journal of Hydrology 594 (2021) 125973

Contents lists available at ScienceDirect

Journal of Hydrology

journal homepage: www.elsevier.com/locate/jhydrol

Research papers

Development of hydro-meteorological drought index under climate change – Semi-arid river basin of Peninsular India

S. Rehana *, G. Sireesha Naidu

Spatial Informatics, International Institute of Information Technology, Hyderabad 500032, India

ARTICLE INFO

This manuscript was handled by Emmanouil Anagnostou, Editor-in-Chief, with the assistance of Yongqiang Zhang, Associate Editor

Keywords:
Hydrometeorological drought
Evapotranspiration
Hydrological modelling
Climate change
SPEI
SRI

ABSTRACT

Univariate meteorological drought indices are inadequate to represent the complexity of hydrological conditions under the intensification of hydrological cycle due to climate change at catchment scale. In this study, Standardised Precipitation Actual Evapotranspiration Index (SPAEI) was proposed, which can combine both meteorological and hydrological drought characteristics at catchment scale. The proposed new drought index considers the hydrologically calibrated AET to account for the water use in addition to meteorological effect. The proposed hydrometeorological drought index was potential in identifying meteorological and hydrological drought events accounting for the time-lag effects and comparable with Global Land Evaporation Amsterdam Model (GLEAM) remote sensing AET data-based drought index. The PET based drought index of SPEI, which is based on energy demand, has shown intensified drought characteristics compared to SPAEI, which is based on both energy demand and available moisture supply and can be a promising variable in the drought estimation. The climate change projections of precipitation and temperatures downscaled using statistical downscaling model based on K-means clustering, Classification and Regression Trees and Support Vector Regression were used using three General Circulation Model outputs. Intensified drought characteristics under climate change has been predicted over Krishna River basin, India, in terms of increase of drought areal extent of about 25%-31%, with increase of drought frequency as 5 years per 20 years and durations as 4–5 months based on the proposed hydrometeorological drought index of SPAEI.

1. Introduction

Drought is one of the most widespread and slowly developing natural hazard due to the lack of water availability in terms of precipitation and consequent shortage of streamflow and soil moisture affecting socio-economics (Aadhar and Mishra, 2017; AghaKouchak et al., 2015; Dai, 2011). It corresponds to the failure of spatial and temporal precipitation (meteorological drought), inadequate streamflows (hydrological drought), decrease in soil moisture and crop yields (agricultural drought), therefore consequent impact on ecosystem and socioeconomic activities of the human being (socio-economic drought) (Wilhite and Glantz, 1985). Among these, the most widely used drought indices at regional scale water resources management are meteorological and hydrological to characterise and compare drought severity, frequency and duration (Marcos-Garcia et al., 2017). A meteorological drought index accounts for the deviation of climatological variables (precipitation and Potential Evapotranspiration (PET)) in a given year from the normal conditions [e.g. Standardized Precipitation Index (SPI)] by (McKee et al., 1993); Standardized Precipitation Evapotranspiration (SPEI) developed by (Vicente Serrano et al., 2010). Nevertheless, none of these meteorological indices can consider the effect of evapotranspiration flux based on actual water availabilities in the drought estimation. Furthermore, such meteorological droughts are independent of actual water availabilities, land use and vegetation in the drought estimation at catchment scale. A drought assessment solely based on meteorological aspects without considering deficits in hydrological cycle will not be sufficient for the regional water resources management decision under climate change (Oloruntade et al., 2017). Whereas, hydrological drought assessment is based on the fall of streamflow and water storages below long-term mean levels [e.g. Standardized Runoff Index (SRI), Shukla and Woods (2008)]. Implementation of such hydrological drought assessments are limited for ungauged basins (Loon et al., 2019). Furthermore, hydrological drought assessment entirely based on below normal streamflow may mislead due to the human influenced regulated flows due to diversions, water transfers and instream abstractions (Lanen et al., 2013). Traditionally, drought

* Corresponding author.
E-mail address: rehana.s@iiit.ac.in (S. Rehana).

https://doi.org/10.1016/j.jhydrol.2021.125973
Received 22 August 2020; Received in revised form 26 November 2020; Accepted 6 January 2021
Available online 12 January 2021

assessment studies were exclusively based on either meteorological or hydrological aspects without considering the combined effect of climatological deviations and acute water shortages at river basin scales. To this end, drought assessment studies have evolved by integrating various meteorological (e.g. SPI) and hydrological drought indicators (e.g. SRI) in a unique manner of aggregation to develop composite drought indices (Shah and Mishra, 2020; Wang et al., 2020). These composite drought indices can combine the individual drought indicators either statistically (e.g. copula based composite drought index, (Shah and Mishra, 2020; Wang et al., 2020) or simple weighting (entropy weighted drought index, Waseem et al., 2015). However, to understand the complexity and time lags (Yang et al., 2017b) between meteorological and hydrological drought indices, it is very important to structure the drought indices with an integration of most prominent hydro-meteorological variables to retain the dependence between these variables. Given the limitations of meteorological and hydrological drought indices as individual, a drought index which will synthesize the hydro-meteorological information can be more reliable in the context of operational drought management at river basin scale under climate change. A comprehensive hydro-meteorological drought index combining major hydrological variables such as precipitation, PET, AET and runoff (R) simultaneously to characterise the meteorological and hydrological drought will be more promising for efficient drought management at catchment scale..

The Standardized Precipitation Evapotranspiration Index (SPEI) has become popular meteorological drought index due to the inclusion of atmospheric climate demand as the difference (P-PET) between Precipitation (P) and Potential Evapotranspiration (PET) (Vicente Serrano et al., 2010). Even though, SPEI has proven to be more reliable measure than Standardized Precipitation Index (SPI) (e.g. Tirivarombo et al., 2018), as it includes PET in addition to P, it cannot account for the actual water availability of a region. Moreover, (P-PET) is energy based atmospheric water demand and do not account for the effects of regional land surface changes and actual moisture availability, which is the difference (P-AET) between P and Actual Evapotranspiration (AET). Also, PET is the maximum possible moisture loss limited only by the energy endowment or it is the energy-driven ET (Shelton, 2008). Whereas, AET represents the transfer of moisture from the surface to the atmosphere in response to both the energy demand and available moisture supply and can be a promising variable in the drought estimation (Liu et al., 2017). Inclusion of AET in meteorological drought indices, such as SPEI, which is a prominent hydrological variable, can represent hydro-meteorological drought indicator. The present study aimed at inclusion of most prominent hydrological variables of P, PET, AET and R in the drought formulation to develop a hydro-meteorological drought indicator which can work accurately to define both meteorological and hydrological aspects together at catchment scale.

The conventional approaches to estimate AET at river basin scales is based on data intensive macro scale distributed hydrological simulation models and water balance methods expressed as AET = P-R, at annual time scale (Hamel and Guswa, 2015). Alternatively, several parametric models have been developed for estimating AET, with operational meteorological variables of precipitation and temperatures as inputs (e.g. Zhang et al., 2004). Such parametric models are based on the assumption that AET is limited by precipitation under very dry conditions and limited by PET under very wet conditions (e.g. Budyko, 1974). However, these parametric models of AET are purely based on region-specific climate considering P and PET and limited to represent variability of evapotranspiration under water uses (Asokan et al., 2010). In this context, time-invariant model parameters were estimated at catchment scale with consideration of closure of water-balance by (Asokan et al., 2010; Jarsjö et al., 2008). However, time-invariant catchment scale parameters are limited to capture temporal variability of water-energy balance variables, instead, dynamic model parameters accounting for the variations of P, PET and R under climate signals with the closure of water balance can be more promising (e.g. Rehana et al., 2020c). Application of such hydrological calibration models on the AET estimates can account for the variability of P, PET and R at catchment scale. Inclusion of such hydrological induced AET in the drought estimation can account for the catchment-scale hydro-meteorological aspects. The present study proposed a modelling framework to include hydrologically calibrated AET estimates in the formulation of SPEI to develop a new hydro-meteorological drought monitoring index, Standardized Precipitation Actual Evapotranspiration Index (SPAEI). It can be noted that, the parametric AET model adopted in the present study is based on Budyko formulation, which is suitable for long-term basin average scale and large catchments (Gunkel and Lange, 2017). Therefore, the study mainly focused on 12-month time scale (annual drought) characterization to avoid the use of short-term soil moisture storages (Donohue et al., 2007). The proposed drought index of SPAEI consider the joint effect of meteorological and actual water budget, and has a potential to evaluate the effects of climate and hydrological changes. In order to study the impacts of climate variability on drought characteristics the study adopted statistical downscaling model-based projections of precipitation and temperature based on General Circulation Model (GCM) outputs. The study compared the newly proposed hydro-meteorological drought index of SPAEI with meteorological drought index of SPEI and hydrological drought index of Standardized Runoff Index (SRI) for current and projected scenarios. The proposed drought index was tested on a semi-arid river basin of peninsular India, Krishna River Basin (KRB).

2. Methodology

2.1. Case study and data

Krishna River Basin (KRB) is the fifth largest river basin in India occupying an area of 2, 58, 948 km^2 which is 8% of the total geographical area of the country within the range 73°17′–81°9′E and 13°10′-19°22′ N (Fig. 1). Most of the basin is covered by semi-arid climate with annual average precipitation as 784 mm, of which approximately 90% occurs during the South West Monsoon from June to October (http://indiawris.nrsc.gov.in/wrpinfo/?title=Krishna). The KRB is with semi-arid climate with aridity index (P/PET) as 0.44, estimated with basin annual average precipitation (778 mm) and PET (1773 mm) for the period from 1951 to 2015. Precipitation is unevenly distributed over the basin, with heavy precipitation over the western Ghats of about 2500 mm of annual average and moderate to less rainfall of about 500 mm of annual average over the districts of Maharashtra and Telangana. Most of the districts covering the basin are drought prone (Source: http://india-wris.nrsc.gov.in/wrpinfo/index.php?title=Krishna). Rhe river basin water of about 61.9 Billion Cubic Meters (BCM)/year is utilised for irrigation purpose (Rooijen et al., 2009). Severe drought events have been experienced in the basin in recent years during the period of 2001 to 2004, where most of the river basin water was committed to human consumptive uses, affected the irrigation water supplies severely. Moreover, the surface water resources were almost entirely committed to human consumptive uses, groundwater was over-abstracted and the discharge to the ocean almost nil (Venot et al., 2008).

Daily precipitation data from India Meteorological Department (IMD) available for the period of 1901–2015 at $0.25^\circ \times 0.25^\circ$ resolution was considered as observed dataset (Pai et al., 2014). The gridded daily mean temperature data from IMD available for the period of 1951–2014 at $1^\circ X 1^\circ$ resolution was used as temperature observational dataset (Srivastava et al., 2009). The temperature was interpolated to $0.25^\circ \times 0.25^\circ$ resolution using the inverse distance weighting method. The daily precipitation and temperature data sets at $0.25^\circ \times 0.25^\circ$ resolution were cropped for Krishna River Basin covering 348 grids. The daily precipitation and temperatures data sets obtained from IMD were aggregated over monthly time scale to serve as primary inputs to calculate SPEI and SPAEI at each grid at $0.25^\circ \times 0.25^\circ$ resolution. The average monthly air temperature data sets were used in the estimation of PET using

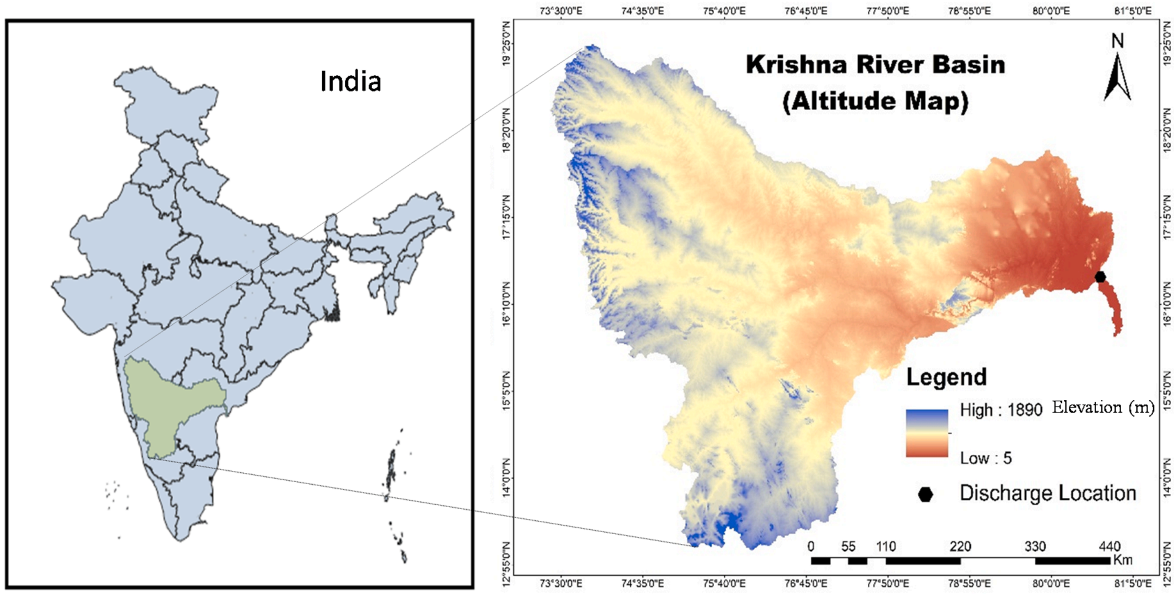

Fig. 1. Map for the Krishna River Basin (KRB), location of the KRB in India and elevation map of the basin showing the discharge location.

Thornthwaite model. Further, the estimated monthly PET and P were forced into the proposed hydrological induced AET modelling framework to estimate the SPAEI drought index.

The Digital Elevation Model (DEM) data with a resolution of 30-arc second (approximately 1 km) was collected from Global 30 Arc-Second Elevation (GTOPO30) dataset provided by USGS (U.S Geological Survey). Using raster extraction in Quantum Geographic Information System (QGIS) the KRB basin was delineated using the DEM data. The discharge data was obtained from Krishna & Godavari Basin Organisation (KGBO), Central Water Commission (CWC), Hyderabad, Government of India (http://www.kgbo-cwc.ap.nic.in) for the basin outlet at gauging station Vijayawada, discharge location for the period of 1966 to 2015.

Further, to study and validate the strength of the proposed hydrometeorological drought index, the present study used satellite-based land surface AET estimates in the drought index formulation. The study adopted Global Land Evaporation Amsterdam Model (GLEAM) satellite-based AET data which provides the land evaporation data considering the evaporation from land, soil, plant surfaces, open-water and transpiration from vegetation along with dynamic land cover information (https://www.gleam.eu/) (Martens et al., 2017; Miralles et al., 2011). Also, GLEAM based AET estimates has showed high skill scores for most of the land-cover types and widely used in the hydrological assessment (Yang et al., 2017a). The AET data encompassing the KRB was extracted from the original dataset at 0.25° spatial resolution and aggregated to a monthly scale for analysis. A common data period of 1980 to 2014 was considered to study the historical drought characterizations including AET.

The National Center for Environmental Prediction/National Center for Atmospheric (NCEP/NCAR) reanalysis data (Kalnay et al., 1996) with a resolution of 2.5° X 2.5° are extracted for a region of 12.5-20° N to 72.5–82.5° E for the period of January 1951 to December 2005. Twenty NCEP grid points fall over the region considered i.e., 12.5-20° N to 72.5–82.5° E. The NCEP data sets of the monthly sea level pressure, air temperature data and predictor set for a period of 39 years (1951–1989) are used for calibrating the statistical downscaling model and the data from 1990 to 2005 are used for validation.

Three GCM experiments were considered to assess the climate change impacts on hydrometeorological droughts over KRB: (1) CanESM2 (The Second-Generation Earth Model) derived from the Canadian Centre for Climate Modelling and Analysis, Canada, with resolution of 2.8 deg × 2.8 deg; (2) MIROC-ESM derived from the Atmosphere and Ocean Research Institute (The University of Tokyo), National Institute for Environmental Studies, and Japan Agency for Marine-Earth Science and Technology Japan, with resolution of 2.8 deg × 2.8 deg; (3) BCC-CSM1-1(m) (The First Generation fully coupled Climate System Model including atmosphere, ocean, land, and sea-ice components and incorporating global carbon cycle and dynamic vegetation cover) derived from the Beijing Climate Centre, China, with resolution of 2.8 deg × 2.8 deg. The Intergovernmental Panel on Climate Change (IPCC) Assessment Report 5 (IPCC, 2007) has defined Representative Concentration Pathways (RCPs) RCP8.5, RCP6, RCP4.5 and RCP2.6, representing the radiative forcing, expressed as Watts/m^2. The present study employed RCP 4.5 as a stabilization pathway, representing atmospheric radiation at 4.5 Watts/m^2 at the end of 2100 (https://www.ipcc-data.org/guidelines/pages/glossary/glossary_r.html).

2.2. Methods

2.2.1. Meteorological drought Index: standardised precipitation Evapotranspiration index (SPEI)

The SPEI was considered as meteorological drought index, which works based on the climatic water balance, the accumulated monthly difference (in mm) between precipitation and PET as follows:

$$D = P - PET \tag{1}$$

where P is the monthly precipitation (mm) and PET is the monthly potential evapotranspiration (mm). The structure of SPEI works with three-parameter log-logistic distribution by fitting the D (Eq. (1)) series following to Vicente-Serrano et al. (2010). The probability density function (pdf) (f(x)) and cumulative distribution function (CDF) (F(x)) of the three-parameter log-logistic distribution is given as follows:

$$f(x) = \frac{\beta}{\alpha}\left(\frac{X-\gamma}{\alpha}\right)^{\beta-1}\left[1+\left(\frac{X-\gamma}{\alpha}\right)^{\beta}\right]^{-2} \tag{2}$$

where α, β and γ are the scale, shape and origin parameters respectively. The parameters of the log-logistic distribution are obtained by following the L-moment procedure as follows:

$$\beta = \frac{2w_1 - w_0}{6w_1 - w_0 - 6w_2} \tag{3}$$

$$\alpha = \frac{(w_0 - 2w_1)\beta}{\Gamma(1 + 1/\beta)\Gamma(1 - 1/\beta)} \tag{4}$$

$$\gamma = w_0 - \alpha\Gamma(1 + 1/\beta)\Gamma(1 - 1/\beta) \tag{5}$$

where w_0,w_1 and w_2 are the probability weighted moments calculated based on Yue and Hashino (2007) as follows:

$$W_r = \frac{1}{n}\left(\frac{n-1}{r}\right)^{-1}\sum_{j=1}^{n-r}\left(\frac{n-1}{r}\right)x_j r = 0, 1, 2 \tag{6}$$

where n is the sample size and x_j is the ordered vector of observations in descending order. Next, the cumulative distribution function of log-logistic distribution can be calculated with the estimated parameters of Pearson-III distribution.

$$F(x) = \left[1 + \left(\frac{X-\gamma}{\alpha}\right)^{-\beta}\right]^{-1} \tag{7}$$

The three-parameter log-logistic distribution was applied to model the time series of (P-PET) for various time scales. Furthermore, the fitted three parameter log-logistic distribution is validated with the Kolmogorov-Smirnov (K-S) (Chakravarti, 1967) goodness of fit test for the climatic water balance time series of D.

With the values of F(x) (Eq. (7)), the SPEI values were calculated as follows:

$$SPEI = W - \frac{C_0 + C_1W + C_2W^2}{1 + d_1W + d_2W^2 + d_3W^3} \tag{8}$$

$$where\ W = \sqrt{-2ln(P)} for\ P \leqslant 0.5 \tag{9}$$

where P is the probability of exceeding a determined D value, P = 1 – F(x). If P > 0.5, then P is replaced by 1- P and the sign of the resultant SPEI is reversed. The constants are Co = 2.5515517, C1 = 0.802853, C2 = 0.010328, d1 = 1.432788, d2 = 0.189269, and d3 = 0.001308, obtained based on Abramowitz (1974), which serve as constants in the conversion of inverse normal distribution function for a given probability value, P. The drought severity of SPEI can be categorization as follows: moderate if SPEI were in between −1.0 to −1.49, severe if SPEI were in between −1.50 to −1.99, and extreme if SPEI were less than −2.0 based on (Vicente-Serrano et al., 2010).

2.2.2. Development of hydro-meteorological drought Index: standardised precipitation actual evapotranspiration index (SPAEI)

The proposed hydro-meteorological drought index, SPAEI, was aimed to integrate most important operational meteorological drought defining variable (P), hydrological drought defining variable (R) at catchment scale. The most complex hydrological variable which define both meteorological and hydrological drought characteristics at catchment scale in terms of water availability (P, R) and evaporative demand (PET) is Actual Evapotranspiration (AET). The present study aimed to include hydrologically induced AET in the structure of SPEI to formulate hydro-meteorological drought indices as shown in Fig. 2. The Fig. 2 shows the overview of the proposed methodology to estimate the hydro-meteorological drought index, SPAEI. The SPAEI considered hydrologically induced AET at catchment scale including meteorological variables of precipitation and temperatures along with hydrological variable of runoff (Fig. 2). First, the PET was estimated with Thornthwaite model (Thornthwaite, 1948) with monthly average air temperature and geographical location of the region of interest as input variables. It can be noted that PET can be estimated using any other standard model, such as Penman-Monteith model, which may require various meteorological variables, such as temperature, wind speed, relative humidity, radiation (Hargreaves and Allen, 2003). Due to the unavailability of observed gridded data sets for the case study, the study limited to use Thornwaite model for the estimation of PET. The next step in the hydro-

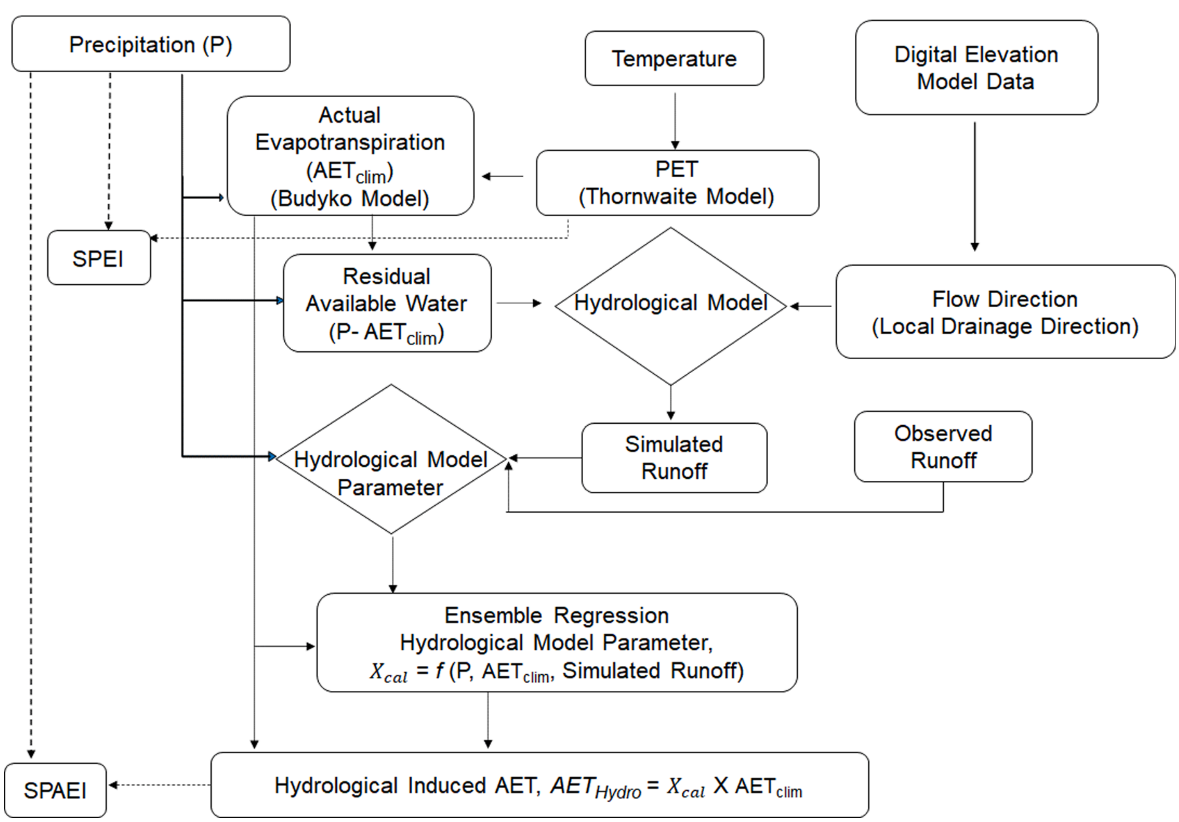

Fig. 2. Over view of the modelling approach to estimate hydro-climatological induced AET at catchment scale.

meteorological drought formulation is the estimation of hydrological induced AET as a function of P, PET and R. One of the classical formulations to estimate AET is Budyko model, which is a function of P, PET and parameter 'ω', which accounts for the non-climatic catchment characteristics (Budyko, 1974) (Eq. (10)).

$$\frac{AET}{P} = 1 + \frac{PET}{P} - \left(1 + \left(\frac{PET}{P}\right)^{\omega}\right)^{(1/\omega)} \tag{10}$$

Here, one of the widely used non-parametric formulation of Budyko equation is developed by (Zhang et al., 2004) for the estimation of AET, as follows:

$$AET_{climate} = \left[P\left(1 - exp\left(\frac{-PET}{P}\right)\right)PETtanh\left(\frac{P}{PET}\right)\right]^{0.5} \tag{11}$$

It should be noted that the Budyko formulation was developed for large catchments (>10000 km^2) at long-term average scale with stationary hydrological conditions as assumptions with negligible soil water storage changes (Gunkel and Lange, 2017; Wu et al., 2017; Yang et al., 2007). In order to guarantee the relevance of AET based catchment scale drought index and to avoid the use of short-term soil moisture storages, the focus of the present study was made at 12-month accumulated annual drought characterization.

The AET can be estimated with the P and PET estimated at monthly time scale using Eq. (11). As the workability of AET model applied in the present study, which is based on Budyko formulation, is more towards annual scales, the study worked to estimate the 12-month scale drought indices. The monthly P and PET are accumulated to 12-month scale as follows:

$$P_i^k = \sum\nolimits_{i-k+1}^{i} P_i \text{wherek} = 12 \tag{12}$$

$$PET_i^k = \sum\nolimits_{i-k+1}^{i} PET_i \text{wherek} = 12 \tag{13}$$

Where $P_i^k$and $PET_i^k$are the accumulated precipitation and PET in month, i. The 12-month accumulated P and PET values will be used in Eq. (11) to estimate the accumulated AET values at 12-month scale. By applying accumulated values of P and PET directly in the Eq. (11), the conditions of P becoming zero for any given month can overcome in the calculation. With this, the study has focused on annual drought index of 12-month accumulation time period. It can be noted that due to seasonality of rainfall, short-term droughts (e.g. 1-month accumulation) can be valuable to evaluate the effect of time lags of precipitation response on hydrological droughts at monthly scale. Such short-term drought duration assessment can be promising for the agricultural water management.

The AET estimated based on Eq. (11) is completely based on meteorological forcing and region-specific climatic conditions and therefore can be considered as climate induced AET (AET_{clim}) (Asokan et al., 2010). Such climate induced AET (with P and PET) cannot account for the variability in evapotranspiration flux under water use changes (with P, PET and R) in the drought estimation (Rehana et al., 2020a) Therefore, AET_{clim} has to be hydrologically calibrated to account for the variability of P, PET and R at catchment scales, which can further serve as input for the hydro-meteorological drought index $SPAEI_{Hydro}$ as shown in Fig. 2. The $AET_{clim,i}$ can be evaluated by integrating the basin runoff, R, to estimate hydrologically induced AET, AET_{Hydro}. For this purpose, single model parameter for the entire river basin at annual time scale has been introduced by Asokan et al. (2010) and Jarsjö et al. (2008), where the observed ($R_{Obs,outlet}$) and uncalibrated ($R_{Calculated,outlet}$) runoff estimated from the hydrological model at the basin outlet were compared as follows:

$$\frac{R_{Calculated,outlet}}{R_{Obs,outlet}} = \frac{P - AET_{clim}}{P - (X_{Cal}{}^*AET_{clim})} \tag{14}$$

$$X_{Cal} = \frac{R_{Obs,outlet}}{R_{Calculated,outlet}} + \left(1 - \frac{R_{Obs,outlet}}{R_{Calculated,outlet}}\right)\frac{\sum P}{\sum AET_{clim}} \tag{15}$$

Where,$R_{Obs,outlet}$ and $R_{Calculated,outlet}$ are the long-term annual average observed and simulated runoff at the basin outlet in m^3/s respectively and $\sum P$ and $\sum AET_{clim}$ are the long-term accumulated annual average observed precipitation and AET estimated based on Eq. (11). over the basin in mm/year. The simulated runoff, $R_{Calculated,outlet}$, will be calculated by dividing the entire river basin into uniform grids. At each grid, i, the Residual Available Water, $RAW_{calculated,i}$ will be estimated using annual total Precipitation (P_i) and climate induced AET ($AET_{clim,i}$) (from Eq. (11)) as follows:

$$RAW_{calculated,i} = P_i - AET_{clim,i} \tag{16}$$

The discharge at the basin outlet ($R_{calculated,outlet}$) was estimated by accumulating the flow at grid cell, i, ($RAW_{calculated,i}$) and from all upstream grid cells ($RAW_{cal,G}$) according to the flow direction of the river and corresponding to the area of each grid cell (A_{Cell}) as follows:

$$R_{calculated,outlet} = \left(RAW_{calculated,i} + RAW_{calculated,G}\right){}^*A_{Cell} \tag{17}$$

The annual scale basin averaged calibration factors estimated based on Eq. (15) can be applied on the AET_{clim} (Eq. (11)) to study the changes of AET under hydro-meteorological or water-use over the river basin. However, such time-invariant single basin model parameters may not be valid to study the possible hydro-climatic variability under climate change (Rehana et al., 2020c). Furthermore, application of such model parameters developed based on historically observed data may limit to capture the temporal variability of hydro-climatic variables under climate signals (Sireesha Naidu et al., 2020). Given that hydrological variables such as P, PET and R have shown pronounced change under climate change due to the intensification of global hydrological cycle, therefore model parameters should also account for such changes. In this context, developing hydrological model parameters which can relate various hydro-climatic variables such as P, ET and observed R can improve the hydrological model performance (López López et al., 2017). Therefore, the study proposed to estimate the dynamic model parameters accounting for the variability of P, PET and observed R. Such developed models can be used further to estimate the model calibration factors for the future scenarios under climate change projections based on statistical downscaling models. One of the major challenge in implementing such framework are limited data and poor understanding of complex relation between the model parameters and hydrological variables. Thus, the study adopted machine learning models based on Ensemble Regression Model (ERM) to relate model parameters and P, PET and observed R. Therefore, a data driven modelling framework, which can relate the model parameter and other hydro-climatic variables such as P, PET and R can be more appropriate following to the study of Rehana et al. (2020c). The present study also adopted dynamic model parameter hydrological induced model parameter (X_{Cal}) accounting for the temporal variability of P, PET, and R, based on Ensemble Regression Model (ER).

2.2.3. Ensemble Regression (ER) model

Ensemble Regression (ER) methods are machine learning paradigms in which multiple methods which are often referred to as weak learners are trained to solve a problem and are combined to get better results (Friedman, 2001). The ER model works on the hypothesis that diverse set of models can make better predictions in comparison with an individual model. The ER models has gained interest in the hydrological model assessments in recent years (Sajedi-Hosseini et al., 2018).

The input training dataset of 'N' points $\{X, Y\} = \{(x_i, y_i)\}_{i=1}^{N}$, where x_i is the set of predictors and y_i as the observed predictand value at the i^{th} timestep will be considered. Initially, all predictors are given equal weighting coefficients (equal importance - $\alpha_i = \frac{1}{N}$) and an initial model ($F_0(x)$) will developed to predict values of the form $y = F_0(x)$.

At every iteration, m, the residuals(r_{im}) will be calculated between observed (y_i) and modeled predictand value ($F_{m-1}(x_i)$) (Friedman, 2001).

$$r_{im} = -\left[\frac{d\left(\sum_{i=1}^{N}[y_i - F_{m-1}(x_i)]^2\right)}{d(F_{m-1}(x_i))}\right] \text{fori} = 1..\text{N} \tag{18}$$

A base-learner (h_m) will be fitted to these residuals using a Loss function 'L' in the direction of steepest gradient i.e weight, α_i of point 'i' is increased corresponding to a higher value of residual using the training set $\{(x_i, r_{im})\}_{i=1}^{N}$. The model is then sequentially updated as follows:

$$F_m(x) = F_{m-1}(x) + argmin_h \sum_{i=1}^{n} L(y_i, F_{m-1}(x) + h_m(x_i, r_{im})) \tag{19}$$

where the $argmin_h$ refers to minimization of base-learner error (h_m) (https://statweb.stanford.edu/~jhf/ftp/trebst.pdf). The least squares loss function $L(y, F(x)) = \frac{1}{2}(y - F(x))^2$ is used to update the residuals (Friedman, 2001).

The annual scale calibration factors (X_{Cal}) were estimated which can be considered as predictand variable (y_i) and uncalibrated runoff (P-AET) resulting from hydrological ($RAW_{calculated,i}$) (Eq. (16)) model along with P and AET were considered as predictor variables (x_i) in training and testing of ER model. Such dynamic model parameter can be applied on the AET_{clim} (Eq. (11)) to study the changes of AET under hydro-meteorological or water-use over the river basin for current and future scenarios.

$$AET_{Hydro} = X_{Cal} * AET_{clim} \tag{20}$$

Where AET_{hydro} represent the hydrological AET representing the evaporative demand of the atmosphere accounting for energy available in terms of PET and water supply in terms of R. The hydrologically calibrated AET estimates can serve as input to the hydro-meteorological drought index of SPAEI along with precipitation as follows:

$$SPAEI_{Hydro} = P - AET_{Hydro} \tag{21}$$

The SPAEI also followed the original structure of SPEI in fitting the time series of ($P - AET_{Hydro}$) using three-parameter log-logistic distribution to formulate annual hydro-meteorological drought index as explained in Section 2.2.1.

2.2.4. Climate change projection Model: Statistical downscaling model (SDM)

To study the climate change impacts on drought characteristics (frequency, severity and duration), the present study integrated the climate change projections of precipitation and temperatures derived based on General Circulation Model (GCM) outputs using a statistical downscaling model. The statistical downscaling models are the state-of-the-art climate change projections prediction models which relates large-scale climate variables (e.g. mean sea level pressure, wind speed) with surface hydrological variables (e.g. precipitation) using statistical methods (Eum et al., 2020). The present study developed a multisite statistical downscaling model to predict the climate change projections of precipitation and temperatures. The basic formulation of statistical downscaling model includes data preprocessing to remove systematic bias in the modeled and actual climate observations (Bias correction), data reduction method (Principal Component Analysis, PCA), predictand variable states estimation (K-means clustering), fitting algorithm to relate predictors and predictand states (CART), transfer function (Support Vector Regression) based on Sireesha Naidu et al. (2020). National Center for Environmental Prediction/National Center for Atmospheric Research (NCEP/NCAR) climate data from 1948 to the present at a resolution of $2.5^{o} \times 2.5^{\circ}$ was considered as large-scale observed climate variables. The potential predictor variables which have shown significant correlation coefficients with precipitation were identified as surface air temperature, wind speed, humidity, etc., which were also found as potential predictors in other studies over India (Rehana and Mujumdar, 2012; Salvi et al., 2013). Spatial resolution mismatch between NCEP and GCM predictor data has been resolved by applying an Inverse Distance Weighting interpolation. The GCM predictor data undergoes bias correction based on Quantile Mapping method by comparing the Cumulative Distribution Functions (CDFs) of NCEP and GCM predictor data for the historical and future scenarios to remove the systematic bias associated with the climate outputs (Li et al., 2010; Salvi et al., 2013). Both bias corrected GCM and reanalysis climate data undergoes with standardization, which involves subtraction of mean and division by standard deviation estimated with all the data points of the time series (Wilby and Dawson, 2013). After data processing, statistically significant climate variables (predictors) were considered to predict the precipitation over various grid points of the basin. To capture the cross-correlation between the grids, rainfall states are defined as dry, moderate and wet. To estimate the rainfall state of the basin, an unsupervised clustering algorithm, K-means clustering was used. K-means clustering is an unsupervised machine learning algorithm that partitions n observations into K clusters for which each observation belongs to the cluster with the nearest mean (Macqueen, 1967). K-means clustering has been widely used in the statistical downscaling models in the prediction of rainfall states (Kannan and Ghosh, 2011). In this study, we used the K-means algorithm to achieve cross correlation among the rain stations and group the months having similar rainfall. This technique reads the observed rainfall values for all grids in the basin in a month, clusters them, and provides a single representative value that is referred to as the state of rainfall for that particular month.

Classification and Regression Tree (CART), which is a decision tree learning technique has been used in categorizing the rainfall into states by building a statistical relation between the continuous principal components extracted from predictor data and the rainfall states estimated using K-means clustering. The established relationship is assumed to intact for the future predictors which are then taken as input for CART model and for which the future rainfall states are estimated. An advantage of CART over linear classification models is that they can capture non-parametric and non-linear relationships as well as yield simple models. Cross validation is carried in order to ensure there is no risk of overfitting the data. For every iteration calculate the Gini's impurity/ diversity Index(E) (Loh, 2011) of the data using the formula given in the equation

$$E = \sum_{i \neq j} P(w_i)P(w_j) = 1 - \sum_{i \neq j} P(w_i)^2 \tag{22}$$

where $P(w_j)$ represents the probability of data being in j^{th} class for each value of the attribute. Choosing an attribute splitting that minimizes the decrease in this impurity (E) as much as possible. It is 0 when all the patterns at node have the same class label. Continue until impurity (E) is less than a certain threshold(η) or on reaching the maximum number of iterations where $E < \eta$.

Individual regression models are built on separating the predictor and observed data based on the weather state category into individual datasets. The SVR model tries to fit the error within a certain threshold (ε), identifying a single separating hyperplane which maximizes the margin rather than solely minimizing the error which helps to find the best model (Vapnik et al., 1997). Linear SVR was used as the regression technique to predict the precipitation and temperature without overfitting. SVR tries to minimize the error of misclassification calculated in addition to maximizing the margin between the separating hyperplane and the support vectors. Application of SVR model in statistical downscaling under climate change can be found in (Gaur et al., 2020; Goly and Teegavarapu, 2020; Rehana, 2019; Sireesha Naidu et al., 2020)

3. Results

The first part of the study tested the performance of the developed hydro-meteorological drought index in capturing the meteorological and hydrological drought characteristics. The second part of the study has focused on quantification of climate change impacts on the proposed hydro-meteorological drought index under precipitation and temperature projections based on statistical downscaling model. More specifically, the study compared the drought characteristics of areal extent, frequency, intensity and duration for the standard drought index of SPEI and proposed hydro-meteorological drought index of $SPAEI_{Hydro}$ under climate change projections.

3.1. Performance of constructed SPAEI

The time series of P-PET and P-AET were fitted with three parameter log-logistic distribution and validated with the Kolmogorov-Smirnov (K-S) (Chakravarti, 1967) goodness of fit test. A rejection frequency for log-logistic distribution was defined as the ratio of number of grid points which did not fit the time series of (P-PET) and (P-AET) with log-logistic distribution, to the total number of grid points in the river basin at a given significance level (Monish and Rehana, 2019). The K-S rejection frequencies for the overall basin including all valid grid points were obtained as 6% and 8% for (P-PET) and (P-AET) respectively at a significance level of 0.05, which are in agreement with earlier studies over KRB (Rehana et al., 2020a).

The Akaike Information Criterion (AIC) (Akaike, 1974) was used to obtain the relative distribution rankings to choose the best suitable probability distribution to fit runoff. The Akaike Information Criterion (AIC) was used to obtain the relative distribution rankings to choose the best suitable distribution to fit runoff. The AIC values for the Lognormal, Generalized Extreme Value (GEV), and Log-Logistic distributions were obtained as 583, 588 and 1783 respectively. Both lognormal and GEV distributions were ranked as the best distributions and the present study used GEV distribution to fit the discharge data in the formulation of SRI due to its better applicability over widely varying hydro-climatic regimes (Shukla and Wood, 2008).

The study tested the superiority of hydro-meteorological drought index of $SPAEI_{Hydro}$ in characterising drought by comparing with SPEI and SRI. The Pearson's correlation coefficients of 12-month scale $SPAEI_{Hydro}$ with SPEI and with SRI from 1966 to 2014 were obtained as 0.73 and 0.76, respectively, which are significant at $p = 0.05$. The Fig. 3. shows the Kendall rank correlation coefficients between SPEI, SRI and $SPAEI_{Hydro}$ at significance test of $\alpha = 0.01$ over KRB at 12-month time scale. It was noted that SPEI and SRI have high correlation coefficients with $SPAEI_{Hydro}$ capturing catchment scale meteorological and hydrological drought characteristics.

The strength of the $SPAEI_{Hydro}$ furthermore investigated based on historical drought events over KRB. Rehana et al. (2020a) pointed out that most severe drought events have occurred in the years of 1972, 1985, 2002 and 2003 over KRB. The effect of $SPAEI_{Hydro}$ was tested by analysing the 12-month scale SPEI, SRI and $SPAEI_{Hydro}$ for the current climatology period of 1966–2014. Table 1 gives the drought intensity for major drought years of 1972, 1985, 2002, 2003 and 2012 estimated based on SPEI, SRI and $SPAEI_{Hydro}$. The 12-month moving time window ending in December can account for both active monsoon and the non-monsoon months over the study area (Mallya et al., 2016), therefore the intensity of major drought years of December months were compared. The drought intensities of hydro-meteorological drought index of $SPAEI_{Hydro}$ were found to be comparable with both meteorological, SPEI, and hydrological, SRI, drought indices intensities. Specifically, for higher runoff value of 17.93 m^3/s in 1985 the SPEI (-1.04) and SRI (-1.21) indices were noted as same with lower intensity of $SPAEI_{Hydro}$ value as −0.65. While, for lowest annual runoff value of 1.07 m^3/s in 2003 the SPEI (-1.16) and SRI (-1.68) indices again same intensities, with higher intensity of $SPAEI_{Hydro}$ as –1.06. With this, $SPAEI_{Hydro}$ can provide a more reasonable catchment scale drought assessment conditions compared to SPEI and SRI (Fig. 4).

To compare the onset and termination of drought events, the study considered −1.0 as threshold. Fig. 5 compares the basin averaged monthly 12-month time scale SPEI, SRI and $SPAEI_{Hydro}$ time series for the period from 1965 to 2015. The years 1972 (a), 1985 (b), 2002 and 2003 (c) and 2012 (d) were noted as major drought years as shown in Fig. 5, exceeding the threshold of −1.0 which is in agreement with earlier research finding over the basin (Rehana et al., 2020a). These were also declared as major drought years all over India (Mallya et al., 2016). The $SPAEI_{Hydro}$ is in agreement with both SPEI and SRI in identifying the major drought events over the basin. For the year 1972 the drought onset with SPEI has started from January-1972 which extended

Table 1
Comparison of drought intensity values and runoff for major drought years over KRB.

Year	SPEI	SRI	$SPAEI_{Hydro}$	Runoff (m^3/s)
1972	−1.24	−1.17	−0.82	15.67
1985	−1.04	−1.21	−0.65	17.93
2002	−1.06	−1.69	−1.26	3.23
2003	−1.16	−1.68	−1.06	1.07
2012	−0.41	−1.48	−1.20	6.53

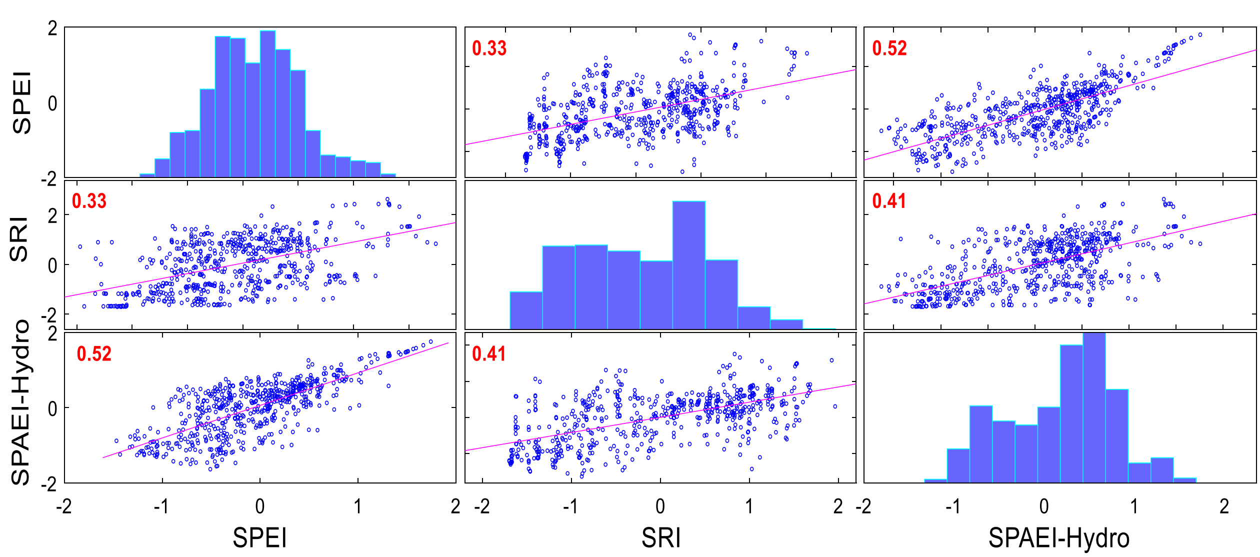

Fig. 3. The Kendall correlation coefficient between SPEI, SRI and $SPAEI_{Hydro}$ estimated for a period of 1951 to 2014 over KRB.

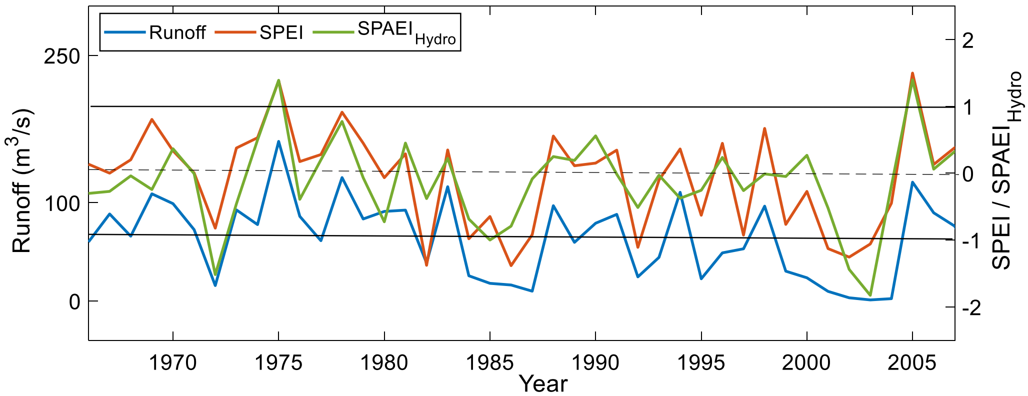

Fig. 4. Comparison of SPEI, $SPAEI_{Hydro}$ and runoff for the period of 1965 to 2007.

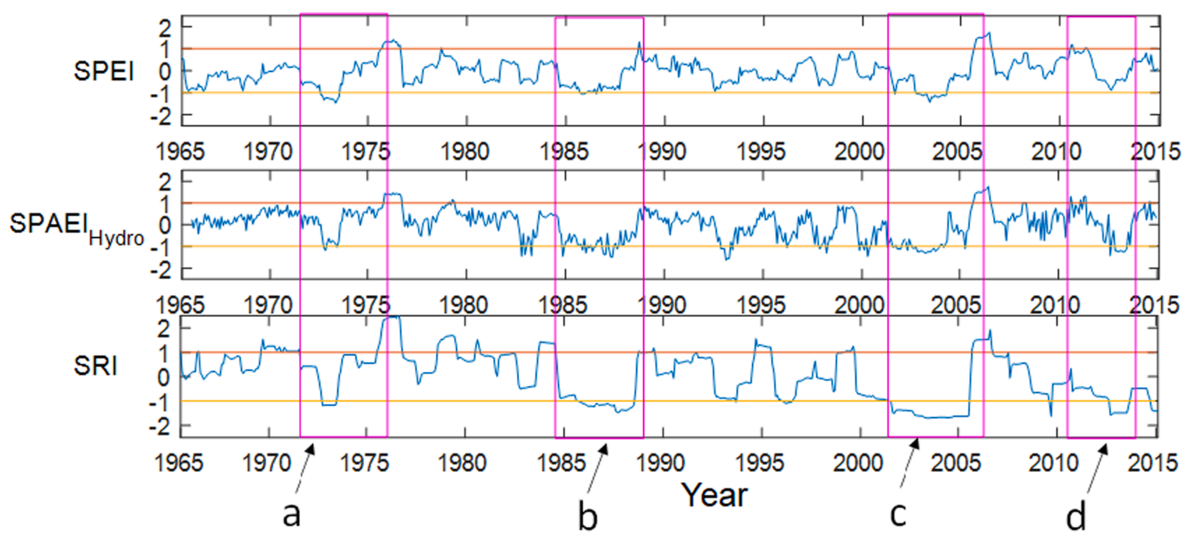

Fig. 5. Comparison between drought intensity of basin averaged SPEI, $SPAEI_{Hydro}$ and SRI series for the period of 1965–2015 of KRB. Major drought years as 1972 (a), 1985 (b), 2002 and 2003 (c) and 2012 (d).

till September-1973. Whereas, the hydrological drought index of SRI has persisted with a time-lag effect for the period of September-1972 to July-1973. The hydro-meteorological drought index, $SPAEI_{Hydro}$, has followed both meteorological and hydrological factors into account and noted drought period from September-1972 to July-1973 as drought onset period with −0.5 as threshold. To illustrate such time-lag effect of meteorological and hydrological drought onsets, the year 1984 which was not a severe drought year, but the SPEI has noted the occurrence of drought from September 1984 with drought intensity as −0.76. However, the SRI has noted the hydrological drought occurrence from October onwards with a time-lag of one month with drought intensity as −0.92. While, the hydro-meteorological drought, has also identified the occurrence of drought from November onwards with drought intensity as −1.46. Overall, $SPAEI_{Hydro}$ was noted to identify the meteorological droughts of SPEI as well as hydrological drought events of SRI for major drought years over the study area accounting for the time-lag effects.

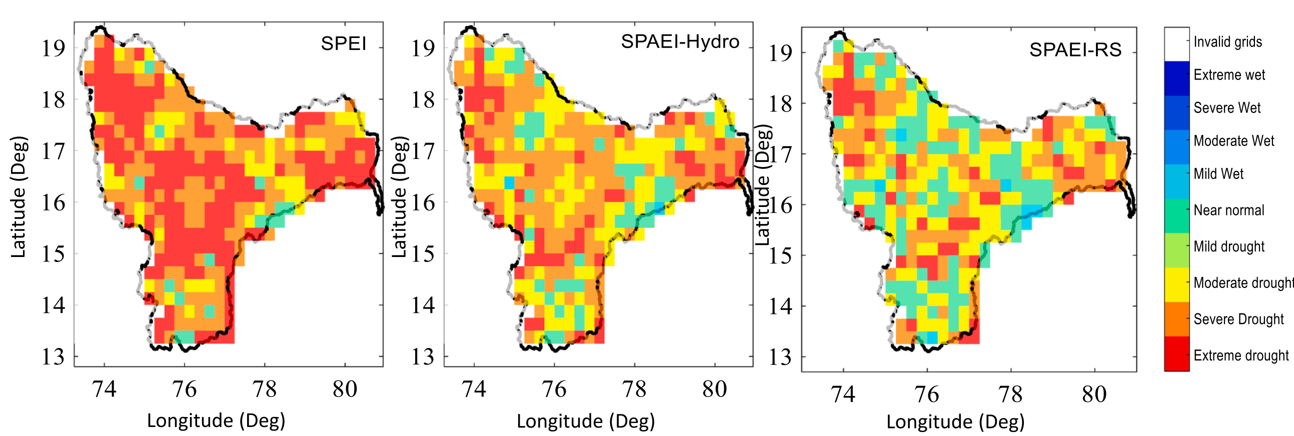

Fig. 6. Drought characterisation for the major drought year of 2002 with SPEI, $SPAEI_{Hydro}$ and SPAEI-RS over KRB.

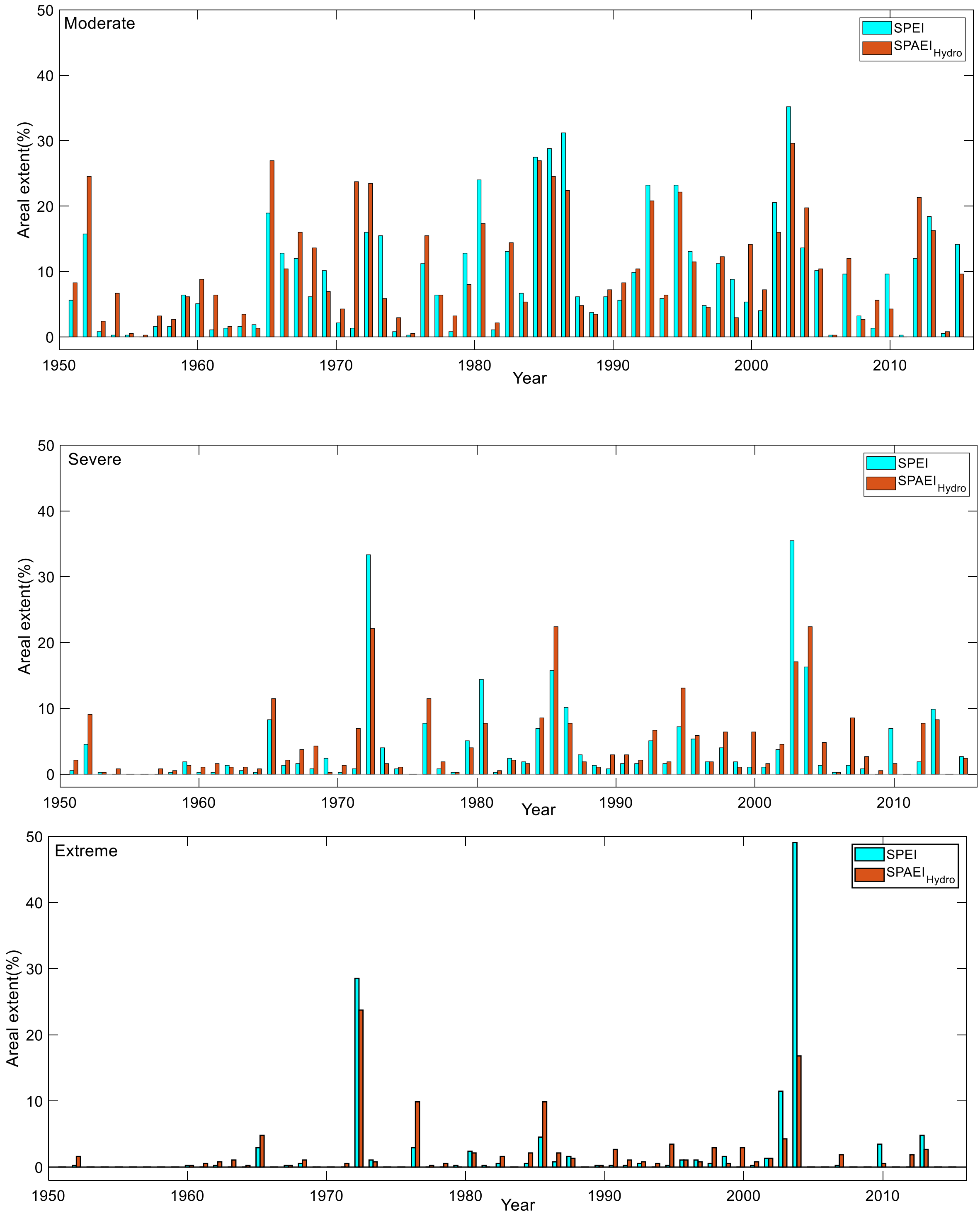

Fig. 7. Drought areal extent (ratio of number of grids affected with moderate, severe and extreme droughts to the total grids covering the entire river basin) with SPEI and $SPAEI_{Hydro}$ estimated for the period of 1951 to 2014 over KRB.

As SPEI is energy-based ET estimate, it is characterizing the drought events as severe compared to $SPAEI_{Hydro}$, which is based on both water availability and energy (Figs. 6 and 7). For example, we considered the most severe drought year of 2002, which was also one of the noted drought all over India (Mallya et al., 2016), for comparing the drought intensity characterization for both SPEI and $SPAEI_{Hydro}$ as shown in Fig. 6. As SPEI was based on the atmospheric water demand without accounting for the terrestrial actual water availability, it has characterized the entire basin under extreme, while $SPAEI_{Hydro}$ has identified as severe and moderate. This can also be noted by comparing the drought areal extents based on SPEI and $SPAEI_{Hydro}$ for various categories of moderate, severe and extreme estimated from 1951 to 2014 as shown in Fig. 7. The areal extent of drought was estimated as the ratio of grids affected with various categories (including moderate, severe and extreme) of drought to the total grid points covering the entire river basin. The SPEI ($SPAEI_{Hydro}$) has characterized 35.2% (29.6%) of area under moderate, 35.47% (17.1%) of area under severe and 49.07% (16.8%) of area under extreme for the drought year of 2002. Therefore,

$SPAEI_{Hydro}$ can provide more insight in capturing the severe and extreme drought characteristics at catchment scales compared to SPEI due to the inclusion of AET in the drought characterizing instead of PET.

Further, to validate the newly proposed hydro-meteorological drought index, we have used remote sensing AET estimates based on GLEAM in the drought formulation of SPEI to frame SPAEI-RS (Fig. 6). The $SPAEI_{Hydro}$ was noted to be more comparable with SPAEI-RS in terms of drought characterization compared to SPEI. It should be noted that the difference between $SPAEI_{Hydro}$ and SPAEI-RS is mainly due to the AET estimation method used in the drought indices formulation. A comparison of modeled AET based on Budyko formulation and remote sensing based AET can be more appropriate to verify the new proposed drought index formulation. The spatial average correlation coefficient between modeled (Budyko) and remote sensing AET data was estimated for a period of 1980 to 2014 and obtained as 0.88. These research findings are in agreement with earlier study by Rehana and Monish (2020), with about 99% of grid points having correlation coefficients >0.8 all over India when compared with the Budyko and GLEAM based AET data sets for period of 1980 to 2014. Overall, the newly proposed hydro-meteorological drought characterization has followed the remote sensing AET based drought index, which is most dependable and validated global terrestrial AET data with many hydrological applications (Zhang et al., 2010).

It can be noted that the SRI estimated is with the basin outlet discharge point, which is always affected by water abstractions. Therefore, the hydrological drought was experienced for almost for all months (Fig. 5). Ideally, the discharge locations for comparison should be considered at sub-basin scale, since, the hydrological model applied in the present study is with closure of water-balance and therefore, basin outlet discharge location was considered in the estimation and comparison of SRI index with SPEI and $SPAEI_{Hydro.}$

3.2. Hydro-meteorological variability: current and future climate signals

3.2.1. Hydro-climatology over KRB for current and future scenarios

The present study used the climate change projections of precipitation and temperatures based on three GCM outputs to study the climate change impacts on hydrometeorological droughts over KRB. The study considered the current climatology as 1951–1989 and 1990–2005, with future projections time slices as 2021–2040, 2041–2060 and 2061–2080 to study the drought characteristics over KRB. Depending on the NCEP resolution, the predictor matrix has considered around 100 (20 gridsX5 predictors) encompassing the entire basin. Considering that there will be a homogeneous pattern among these predictor variables as well as keeping the computational constraints in view, PCA was applied in order to reduce the problem of multidimensionality and multicollinearity. For capturing 98% of variability of predictor data about 15 principal components have been selected instead of 100 predictor dimensions covering the entire basin in the statistical downscaling model. The rainfall states for the current period were obtained for the observed historical data using K-means clustering which are then given as inputs to CART model to find the rainfall states for GCM future datasets. Then, individual regression model based on SVR were built for each grid for every state. Finally depending on the rainfall state of a month in the future, for every grid the corresponding regression model was identified and applied to get the amount of rainfall in that month. For temperature, a single regression model was built for each grid in contrast to multiple models for rainfall which was applied to get the future temperature predictions. The historical time period of 1951–1989 and 1990–2005 were used as training and testing of the statistical downscaling model. The basin averaged mean values of estimated precipitation and temperatures for training, testing and for the future time periods of 2021–2040, 2041–2060 and 2061–2080 were provided in Table 2 for the observed and for three GCM projections with RCP 4.5 scenario.

The increase in precipitation and temperatures for the future scenarios were predicted compared with the observed time periods (Table 2). The BCCCSM, CanESM and MIROC GCMs have shown lower precipitation averages compared to the observed data but an increase of 16.13 mm to 108.1 mm compared to the historical projections and an increase of 0.55 °C to 0.94 °C in temperatures. There is an average increase of precipitation with about 3.38%, 4.2% and 4.1% with BCCCSM, CanESM and MIROC models respectively over KRB for the future scenarios of 2021–2080 compared to observed period of 1990–2005. Similarly, an increase of temperature of about 0.59, 0.37 and 0.32 °C with BCCCSM, CanESM and MIROC models respectively over KRB for the future scenarios of 2021–2080 compared to observed period of 1990–2005. Such increase of temperature and precipitation results was found to be in comparison with earlier research findings over the basin (Rehana et al., 2020b). For instance, based on Regional Circulation Model (RCM) based Coordinated Regional Downscaling Experiment (CORDEX) projections of precipitation and temperatures were analysed over KRB by Rehana et al. (2020b). Their study noted about 2.19% of increase in precipitation and about 1.29 °C of increase in temperature for the period of 2021–2040 and 2041–2060 respectively compared to observed period of 1966–2003 with RCP 4.5 scenario with various CORDEX model outputs. Compared to RCM projections the GCM projections based on statistical downscaling model as developed in the present study has shown lower precipitation and temperature increases

Table 2
Spatial average annual precipitation and temperatures for current period (1951–1989 (Training), 1990–2005 (testing) and future periods (2021–2040, 2041–2060, 2061–2080) over KRB.

Hydrological Variable	GCMName	Current Training	Validation	Future 2021–2040	2041–2060	2061–2080
Average Annual Precipitation(mm)	Observed	763.06	812.04	–	–	–
	NCEP	663.68	611.83	–	–	–
	BCCCSM	652.39	665.97	668.52	666.65	741.15
	CanESM	636.38	653.93	693.3	744.26	744.5
	MIROC	650.57	648.26	646.13	695.67	735.91
Annual Temperature (^{0}C)	Observed	26.26	26.54	–	–	–
	NCEP	26.25	26.42	–	–	–
	BCCCSM	26.26	26.38	27.03	27.16	27.20
	CanESM	26.17	26.29	26.72	26.93	27.08
	MIROC	26.27	26.20	26.95	26.79	26.85
Annual Potential Evapotranspiration (mm)	Observed	1772.31	1831.13	–	–	–
	BCCCSM	1716.91	1758.94	1917.32	1965.66	1970.01
	CanESM	1712.73	1741.71	1871.67	1932.98	1971.68
	MIROC	1717.49	1697.60	1909.87	1859.31	1868.61
Annual Calibrated Actual Evapotranspiration (mm)	Observed	340.22	495.96	–	–	–
	BCCCSM	571.62	611.81	611.43	621.58	674.76
	CanESM	564.31	594.07	654.35	710.18	684.63
	MIROC	575.09	592.16	580.63	613.75	648.49

over KRB. It can be noted that statistical downscaling models based on GCM outputs have provide more accurate climate change projections as they are developed based on the historical relationship between the large-scale climate and surface based hydrological variables (Eden et al., 2014). From the comparison of the performance of GCM simulations with observed data, the GCM projections which are based on the statistical relationships developed based on the observed climate have proven to be promising tools for the hydrometeorological drought impact assessment over KRB.

The average annual PET estimated with future scenarios of precipitation and temperatures using Thornthwaite model were noted to increase in the range of 100 mm to 200 mm over KRB. There is an average increase of PET with about 6.6%, 5.2% and 2.6% with BCCCSM, CanESM and MIROC models respectively over KRB for the future scenarios of 2021–2080 compared to observed period of 1990–2005. There is a consequent increase in the estimates of AET_{Hydro} in the range of 250 mm to 500 mm compared with the current period as given in Table 2. There is an average increase of hydrological induced AET with about 28.2%, 37.7% and 23.9% with BCCCSM, CanESM and MIROC models respectively over KRB for the future scenarios of 2021–2080 compared to observed period of 1990–2005.

3.2.2. Drought projections based on $SPAEI_{Hydro}$

The precipitation and temperature projections were used as input into the hydrometeorological droughts assessment over KRB in terms of SPEI and $SPAEI_{Hydro.}$ To show the meteorological, hydrological and hydro-meteorological drought impacts under climate change the present study used SPEI, SRI and $SPAEI_{Hydro}$ for current and future scenarios for three GCM outputs. We estimated SPEI, SRI and $SPAEI_{Hydro}$ for all three GCMs for RCP 4.5 scenarios for KRB with downscaled projections of precipitation and temperatures along with the hydrologically calibrated AET and simulated runoff. Before applying any climate model simulation for impact assessment study, the predictability of the hydrometeorological phenomenon has to be tested with observed data for the current climatology (Li et al., 2010). To study the capability of the downscaled climate projections of precipitation and temperatures in predicting for the historical drought periods the three different GCM model outputs in capturing the drought intensities were examined. The study compared the basin averaged SPEI, SRI and $SPAEI_{Hydro}$ based drought intensities for the observed period and with three GCM model outputs as shown in Fig. 8. All three GCMs were able to capture the major historical drought years between the period of 1951 to 2015. For example, the BCCCSM has identified the major drought year of 1972 with SPEI (-1.6), SRI (-1.5) and $SPAEI_{Hydro}$ (-1.32), whereas, The MIROC also has identified the drought year of 1972 with SPEI (-1.4), SRI (-0.11) and $SPAEI_{Hydro}$ (-1.3) as drought intensities. However, canESM model characterised the 1972 with drought intensities with SPEI (0.0), SRI (-1.5) and $SPAEI_{Hydro}$ (-1.3). Overall, BCCCSM and MIROC have identified major drought years over KRB with all three indices of SPEI, SRI and $SPAEI_{Hydro}$ compared to canESM.

The study considered the current climatology as 1951–1989 and 1990–2005, with future projections time slices as 2021–2040, 2041–2060 and 2061–2080 to study various drought characteristics in terms of intensity, areal extent, frequency and duration over KRB (Figs. 8, 9, 10 and 11). Mainly, the study compared the SPEI and $SPAEI_{Hydro}$ drought indices in terms of intensity and areal extent for future scenarios to quantify the impacts on meteorological and hydrometeorological droughts. The moderate and severe drought areal extents have been predicted to increase for the future periods compared to the current. However, the extreme drought areal extent has not been captured attributed to the caveat of statistical downscaling models ability to capture the extremes effectively compared to mean climate (Rehana and Mujumdar, 2012). Overall, the drought area has increased from 14.8% to 23%-44% for the 2021–2040 period, 14%-39% for the 2041–2060 period and 15.4%-30.75% for the 2061–2080 period, there is a net increase of 25%-31% from the current to future periods over KRB (Fig. 9).

Here, drought is analysed in terms of average intensity estimated over the whole basin, frequency of droughts for every time period considered, as well as the average duration of drought in the considered time period. Higher and more frequent drought intensities have been observed with BCCCSM and MIROC with a threshold of '-1' compared to the current periods, particularly after 2000 year. However, the drought intensity is not as high for the severe and extreme drought years compared to the IMD data as the extremes are not captured accurately using the climate change projections of statistical downscaling models.

The frequency of drought is more with SPEI compared to the drought frequency with $SPAEI_{Hydro}$ for most of the basin and higher for the northern regions of the KRB (Fig. 10). The average drought frequency for the current period 1951–2014 was estimated as 9.5 and 9 years

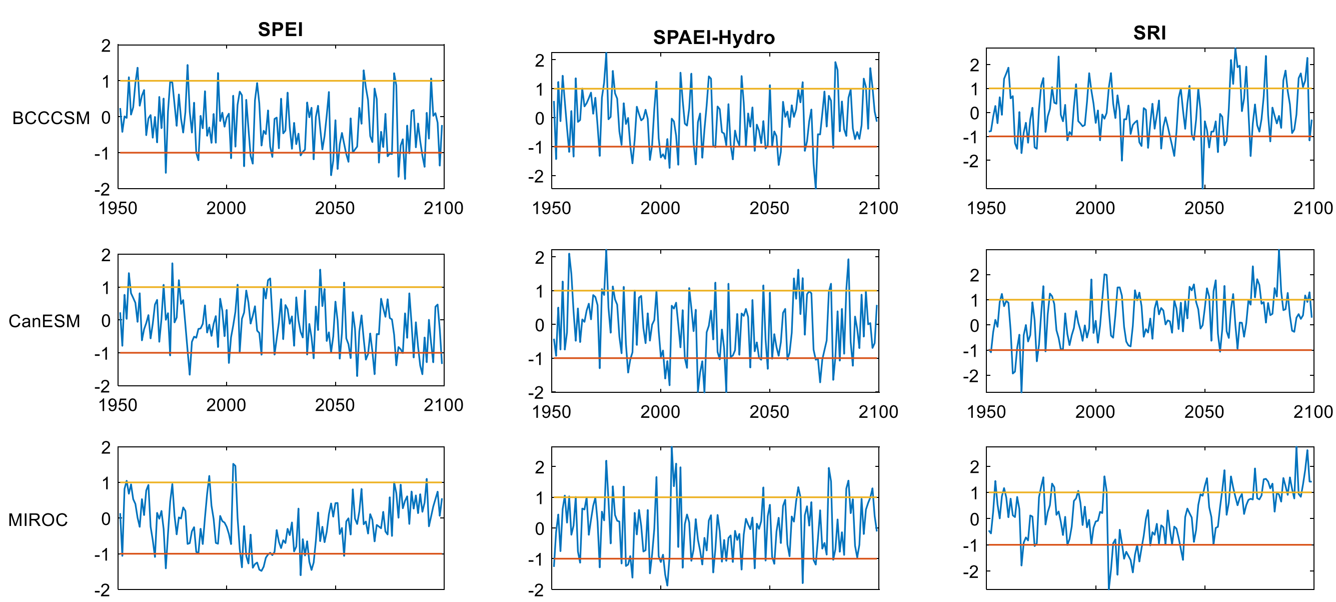

Fig. 8. Comparison of drought intensity of basin averaged (a) SPEI, (b) $SPAEI_{Hydro}$ and (c) SRI for three GCMs BCCCSM, CanESM, MIROC for the time period 1950–2100.

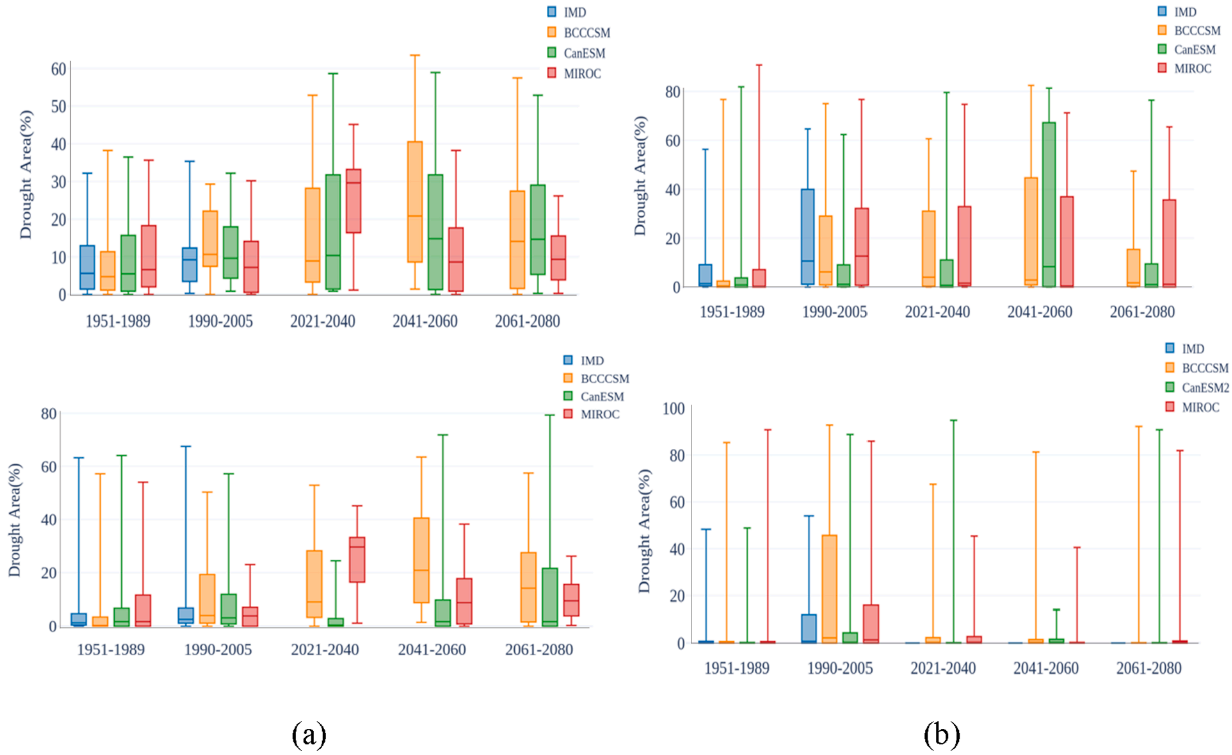

Fig. 9. Comparison of moderate (upper), severe and extreme (lower) drought area estimated with SPEI (a) and $SPAEI_{Hydro}$(b) indices based on observed and various GCM projections for the current and future periods.

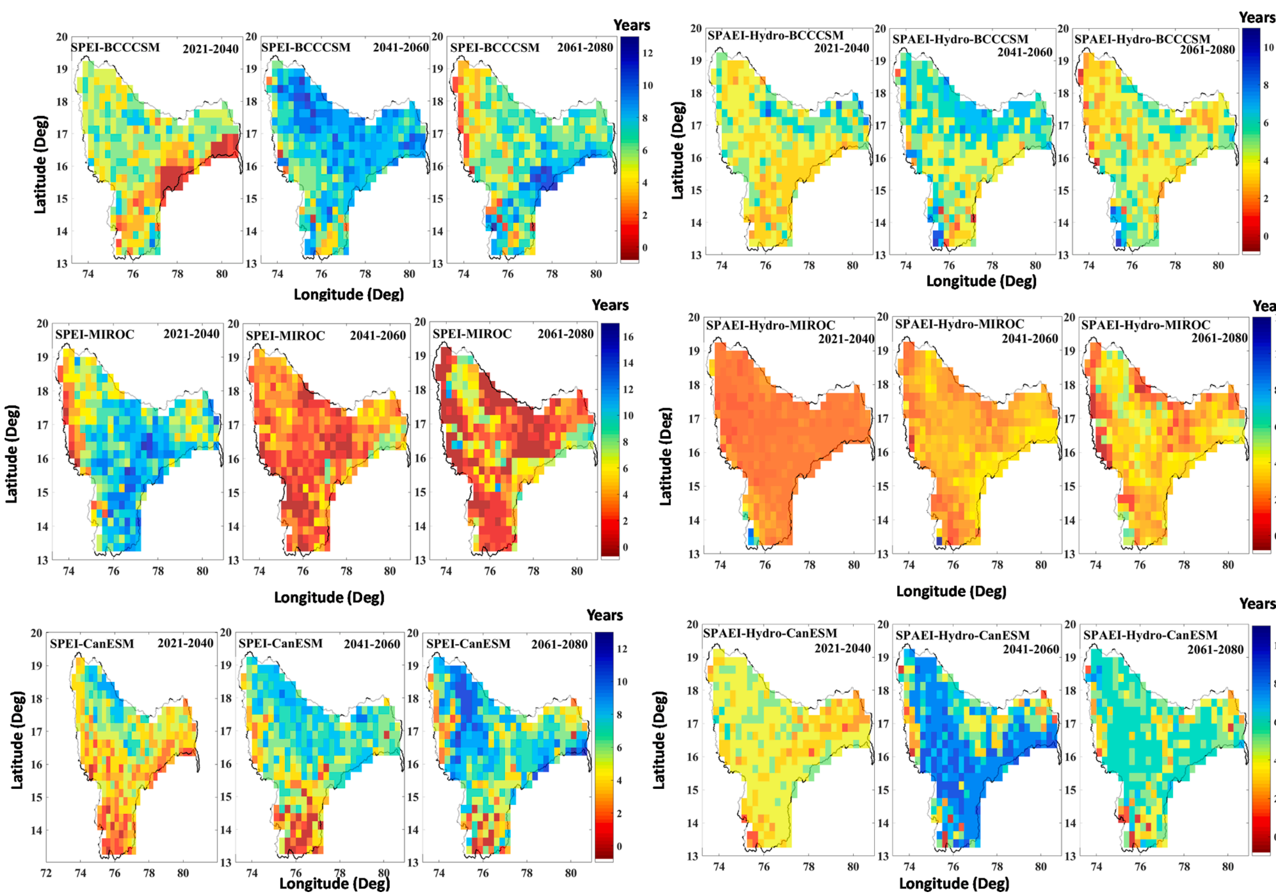

Fig. 10. Frequency of Drought Occurrence (in years) over KRB for the three GCMs of BCCCSM, MIROC, CanESM with SPEI and $SPAEI_{Hydro}$ for three time periods of 2021–2040, 2041–2060 and 2061–2080.

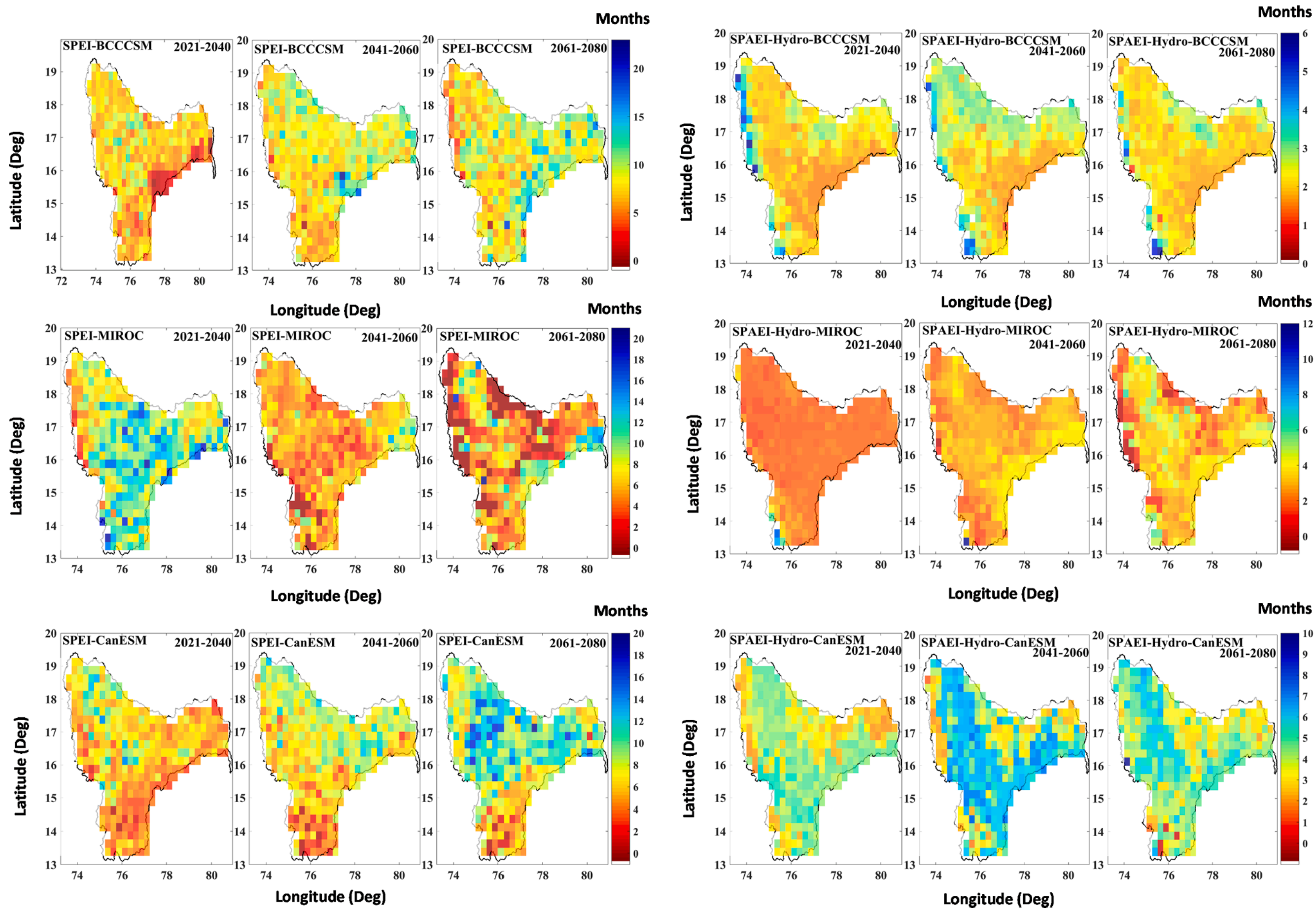

Fig. 11. Drought duration (in months) over KRB for the three GCMs of BCCCSM, MIROC, CanESM with SPEI and $SPAEI_{Hydro}$ for three time periods of 2021–2040, 2041–2060 and 2061–2080.

respectively with SPEI and $SPAEI_{Hydro}$. The study noted that number of drought years were predicted to increase from 5 to 6 years for every 20 years with SPEI. Whereas, the number of drought years increase is predicted with $SPAEI_{Hydro}$ as 4.5 years for every 20 years. Among these projections, the BCCCSM has shown higher drought frequencies for the period of 2041–2060 over the north of the basin with both indices of SPEI and $SPAEI_{Hydro}$. The MIROC has predicted more droughts in the 2021–2040 period with SPEI in the central region of the basin and for both 2021–2040 as well as the period 2061–2080 with $SPAEI_{Hydro}$ in the north western region. However, CanESM has shown higher drought frequencies in the southern parts of the basin with $SPAEI_{Hydro}$ for the period 2041–2060.

The BCCCSM model has predicted the basin averaged drought frequencies with SPEI ($SPAEI_{Hydro}$) as 5 (4), 8 (5) and 6 (4) years respectively for the three future time slices 2021–2040, 2041–2060 and 2061–2080. The basin average drought frequency with MIROC with SPEI ($SPAEI_{Hydro}$) was predicted as 9 (4.5), 3(4), and 3 (5) years respectively for the three future time slices 2021–2040, 2041–2060 and 2061–2080. Following this, the CanESM also has predicted increase of drought frequencies with basin averaged frequencies with SPEI ($SPAEI_{Hydro}$) as 4 (4), 5.7 (6.7), and 6.5 (5) years respectively for the three future time slices 2021–2040, 2041–2060 and 2061–2080. Overall, highest number of droughts were predicted during the time period of 2061–2080 with both SPEI and $SPAEI_{Hydro}$ drought indices, which directs for the possible adaptive measures and policy making for the water resources management over KRB.

Longer drought duration months were noted with SPEI compared to $SPAEI_{Hydro}$ for all over KRB. The basin averaged drought durations were estimated with SPEI and $SPAEI_{Hydro}$ for the current period as 6 and 3 months respectively. As the SPEI is based on the difference between climatic water balance of (P-PET), such long durations can be expected. Such results are evident due to the positive climatic demand with PET (P-PET) resulting in more drought months. Whereas, $SPAEI_{Hydro}$ is based on the hydrological induced AET, involving runoff, along with the precipitation, the lack of water can be expected for few months only compared to atmospheric water demand (P-PET). Therefore, the drought durations were estimated as less for $SPAEI_{Hydro}$ compared to SPEI over KRB.

The drought durations were compared for SPEI and $SPAEI_{Hydro}$ for current and future scenarios based on three GCM climate change projections and compared as shown in Fig. 11. For about 7–9 (2–3) months of basin averaged drought durations were predicted for the period of 2021–2080 with BCCCSM. Whereas, the MIROC model has shown higher drought durations with about 10, 5 and 5 months with SPEI respectively for the period of 2021–2040, 2041–2060 and 2061–2080 with an increase of 1.5–3.5 months with $SPAEI_{Hydro}$. Whereas, the drought duration has been predicted to increase from 6 to 9 (4–5) months with SPEI ($SPAEI_{Hydro}$) for the future scenarios of up to 2060. Overall, drought durations were predicted to increase over the basin for the time period of 2061–2080 with both the drought indices predominantly in the northern parts of the basin which can directly affect the crop productivity and food security.

4. Discussion

The study aimed to include AET in the drought characterisation along with precipitation at catchment scale to represent both hydrological and meteorological aspects combinedly. Whereas, AET is a complex hydrological variable to estimate in comparison to other forms of hydrological variables such as precipitation, runoff and PET. There are various advanced state-of-the-art satellite based remote sensing observations of AET which are available at various spatial and temporal resolutions. However, drought index developed based on such data cannot be used to quantify the impacts of climate change projections on droughts based on the most sophisticated and reliable GCM outputs. Therefore, the study aimed to include AET which was estimated as a function of readily available, estimated and simulated hydro-climate variables (P, R and PET), which can be further used in the drought impact assessment under climate change. For this purpose, the study adopted a well-known and classical approach of AET estimation which was accepted globally for long-term and at catchment scales. The study adopted a calibration-free formulation of Budyko hypothesis to estimate the AET at catchment scale as a function of accumulated P and PET at 12-month scale to frame annual drought estimation. Inclusion of AET in the drought characterisation can account for the transfer of moisture from the surface to the atmosphere in response to both the energy demand and available moisture supply and can be a promising variable in the drought estimation (Liu et al., 2016).

Given the advantages of the proposed drought index, some caveats are still there, which need special attention. Starting with the AET empirical model to statistical downscaling model, there can be several uncertainties arising from various sources. It should be noted that Budyko formulation has been developed for long-term average and large catchments with stationary assumptions towards soil water storage changes due to ground water recharge and human interactions (Gunkel and Lange, 2017). Therefore, the proposed methodology of Budyko formulation of AET estimates for any catchment should be implemented through accurate validation with water balance and most dependable state-of-the-art satellite based AET estimates. Further, the study used Budyko based empirical formulation to estimate AET and one can use any such model (e.g. Turc, 1954) and can study the uncertainty in the drought characterisation.

One of the major assumptions made in the analysis is that AET estimates were at 12-month accumulation monthly time scale by neglecting the storage changes, which are prominent at monthly time scale. The study is limited for the annual drought indices estimation by neglecting the storage changes which can be further extended with the inclusion of appropriate storage component in drought estimation which can definitely account for the agricultural drought aspects at catchment scales.

The AET estimates was used in a conceptual hydrological model involving P and AET to quantify the water availability with closure of water-balance calibration factors in the drought characteristics. The advantage of use of a conceptual hydrological model as implemented in the present study has allowed to use the most prominent hydrometeorological variables which can be modelled and estimated based on the most dependable climate change projections of precipitation and temperatures. The study adopted a dynamic calibration approach which was modelled as a function of P, AET and R using a data-driven algorithm based on Ensemble Regression. The calibrated factors were imposed on the AET estimates based on Budyko framework to estimate the hydrological induced AET, which was used in the hydro-meteorological drought index formulation using the structure of SPEI. Furthermore, we have introduced a calibration parameter only on the AET estimates in the water balance equation of (P-AET). One can extend such basic conceptual model by introducing various other variables such as soil, land use, etc. and can introduce more parameters. Furthermore, the dynamic calibration factor modelled by Ensemble Regression model can be implemented by various machine learning algorithms accounting for such multiple calibration parameter into account. Such modelled calibration factors were further used to estimate the dynamic calibration parameters for the future scenarios with climate change projections of P, AET and uncalibrated runoff. The formulated drought index with hydrologically calibrated AET estimates in SPEI was named as Standardised Precipitation Actual Evapotranspiration Index ($SPAEI_{Hydro}$). The study adopted a statistical downscaling model to generate the climate change projections of precipitation and temperatures with three GCMs with RCP 4.5 scenarios. The study used the newly formulated drought index of $SPAEI_{Hydro}$ to study the climate change impacts on hydrometeorological drought assessment at river basin scale. The study compared the meteorological (SPEI), hydrological (SRI) and hydrometeorological ($SPAEI_{Hydro}$) drought impacts under climate change by integrating the projections of precipitation and temperatures.

It can be noted that the proposed hydro-meteorological drought index is not accounting for the groundwater component of the hydrological system. However, based on sufficient data availability of ground water storage at river basin scale and with the use of basic water balance equation one can account for the ground water component in the proposed drought index. With the inclusion of ground water component in the basic formulation of hydro-meteorological drought index (Eq. (21)) along with P, AET and R, all major forms of droughts such as meteorological, hydrological and agricultural can be represented with one drought index.

The proposed hydrometeorological drought indicator has provided promising results in reconstruction of earlier major drought years over the basin based on both meteorological and hydrological indices accounting for the time-lag effects of both indices. Further, given the advantage to capture both meteorological and hydrological aspects together in one index, the proposed formulation can provide an ease in the water resources management and decision making for the policy makers.

5. Conclusions

The following conclusions are derived from this study:

- The $SPAEI_{Hydro}$ can provide more insight in capturing the severe and extreme drought characteristics at catchment scales compared the SPEI due to the inclusion of hydrologically induced AET in the drought characterizing instead of PET.
- There is an average increase of precipitation (temperature) with about 3.38% (0.59 °C), 4.2% (0.37 °C) and 4.1% (0.32 °C) with BCCCSM, CanESM and MIROC models respectively over KRB for the future scenarios of 2021–2080 compared to observed period of 1990–2005.
- There is an average increase of PET (AET) with about 6.6% (28.2%), 5.2% (37.7%) and 2.6% (23.9%) with BCCCSM, CanESM and MIROC models respectively over KRB for the future scenarios of 2021–2080 compared to observed period of 1990–2005.
- Intensification drought characteristics under climate change over KRB has been predicted in terms of drought areal extent increase of about 25%-31%, with increase of drought frequency as 5 years and durations as 4–5 months based on the proposed hydrometeorological drought index of $SPAEI_{Hydro}$.
- The projected drought characteristics based on SPEI are more intensified compared to $SPAEI_{Hydro}$ due to the consideration of PET, which is maximum possible moisture loss based on energy demand. On the other hand, inclusion of AET as demonstrated in the present study can account for the transfer of moisture from the surface to the atmosphere in response to both energy demand and available moisture supply and can be a promising variable in the drought estimation.

CRediT authorship contribution statement

S. Rehana: Conceptualization, Methodology, Writing - original draft, Investigation, Funding acquisition, Supervision. **G. Sireesha Naidu:** Data curation, Software, Visualization.

Declaration of Competing Interest

The authors declare that they have no known competing financial interests or personal relationships that could have appeared to influence the work reported in this paper.

Acknowledgements

The research work presented in the paper is funded by Science and Engineering Research Board (SERB), Department of Science and Technology, Government of India through Start-up Grant for Young Scientists (YSS) Project no. YSS/2015/002111 to Dr. S. Rehana. We sincerely acknowledge the India Meteorological Department (IMD) for providing the gridded observations of precipitation and temperatures and details of data are given in the website at https://iridl.ldeo.columbia.edu/SOURCES/.IMD/index.html?Set-Language = en. The authors sincerely thank the Editor and three anonymous reviewers for reviewing the manuscript and providing insightful comments.

References

Aadhar, S., Mishra, V., 2017. High-resolution near real-time drought monitoring in South Asia. Sci. Data 4, 1–14. https://doi.org/10.1038/sdata.2017.145.
Abramowitz, M., 1974. Handbook of Mathematical Functions, With Formulas, Graphs, and Mathematical Tables, Dover Publications, Inc., USA.
AghaKouchak, A., Feldman, D., Hoerling, M., Huxman, T., Lund, J., 2015. Water and climate: recognize anthropogenic drought. Nature 524 (7566), 409–411. https://doi.org/10.1038/524409a.
Akaike, H., 1974. A new look at the statistical model identification. IEEE Trans. Automat. Contr. 19 (6), 716–723. https://doi.org/10.1109/TAC.1974.1100705.
Asokan, S.M., Jarsjö, J., Destouni, G., 2010. Vapor flux by evapotranspiration: effects of changes in climate, land use, and water use: vapor flux by evapotranspiration. J. Geophys. Res. 115 (D24) https://doi.org/10.1029/2010JD014417.
Budyko, M., 1974. Climate and life. Academic Press, New York.
Chakravarti, I.M.R.G.L.J.R., 1967. Handbook of Methods of Applied Statistics, 1967 edition/volume I Only edition. ed. John Wiley & Sons.
Dai, A., 2011. Drought under global warming: a review: drought under global warming. WIREs Clim. Change 2 (1), 45–65. https://doi.org/10.1002/wcc.81.
Donohue, R.J., Roderick, M.L., McVicar, T.R., 2007. On the importance of including vegetation dynamics in Budyko's hydrological model. Hydrology and Earth System Sciences 11, 983–995. https://doi.org/10.5194/hess-11-983-2007.
Eden, J.M., Widmann, M., Maraun, D., Vrac, M., 2014. Comparison of GCM- and RCM-simulated precipitation following stochastic postprocessing. J. Geophys. Res. Atmos. 119 (19), 11,040–11,053. https://doi.org/10.1002/2014JD021732.
Eum, H.-I., Gupta, A., Dibike, Y., 2020. Effects of univariate and multivariate statistical downscaling methods on climatic and hydrologic indicators for Alberta, Canada. J. Hydrol. 588, 125065. https://doi.org/10.1016/j.jhydrol.2020.125065.
Friedman, J.H., 2001. machine. Ann. Statist. 29 (5), 1189–1232. https://doi.org/10.1214/aos/1013203451.
Gaur, A., Schardong, A., Simonovic, S.P., 2020. Gridded extreme precipitation intensity–duration–frequency estimates for the Canadian landmass. J. Hydrol. Eng. 25 (6), 05020006. https://doi.org/10.1061/(ASCE)HE.1943-5584.0001924.
Goly, A., Teegavarapu, R.S.V., 2020. Optimization and variants of quantile-based methods for bias corrections of statistically downscaled precipitation data. J. Hydrol. Eng. 25 (7), 04020027. https://doi.org/10.1061/(ASCE)HE.1943-5584.0001926.
Gunkel, A., Lange, J., 2017. Water scarcity, data scarcity and the Budyko curve—an application in the lower Jordan river basin. J. Hydrol.: Reg. Stud. 12, 136–149. https://doi.org/10.1016/j.ejrh.2017.04.004.
Hamel, P., Guswa, A.J., 2015. Uncertainty analysis of a spatially explicit annual water-balance model: case study of the Cape Fear basin, North Carolina. Hydrol. Earth Syst. Sci. 19, 839–853. https://doi.org/10.5194/hess-19-839-2015.
Hargreaves, G.H., Allen, R.G., 2003. History and evaluation of hargreaves evapotranspiration equation. J. Irrig. Drain Eng. 129 (1), 53–63. https://doi.org/10.1061/(ASCE)0733-9437(2003)129:1(53).
IPCC, 2007. Climate change 2007: impacts, adaptation, and vulnerability. In: Parry ML et al (eds) Contribution of working group II to the third assessment report of the intergovernmental panel on climate change.
Jarsjö, J., Shibuo, Y., Destouni, G., 2008. Spatial distribution of unmonitored inland water discharges to the sea. J. Hydrol. 348 (1-2), 59–72. https://doi.org/10.1016/j.jhydrol.2007.09.052.
Kalnay, E., Kanamitsu, M., Kistler, R., Collins, W., Deaven, D., Gandin, L., Iredell, M., Saha, S., White, G., Woollen, J., Zhu, Y., Chelliah, M., Ebisuzaki, W., Higgins, W., Janowiak, J., Mo, K.C., Ropelewski, C., Wang, J., Leetmaa, A., Reynolds, R., Jenne, R., Joseph, D., 1996. The NCEP/NCAR 40-Year reanalysis project. Bull. Amer. Meteor. Soc. 77, 437–472. 10.1175/1520-0477(1996)077<0437:TNYRP>2.0.CO;2.
Kannan, S., Ghosh, S., 2011. Prediction of daily rainfall state in a river basin using statistical downscaling from GCM output. Stoch. Environ. Res. Risk Assess. 25 (4), 457–474. https://doi.org/10.1007/s00477-010-0415-y.
Lanen, H.A.J.V., Wanders, N., Tallaksen, L.M., Loon, A.F.V., 2013. Hydrological drought across the world: impact of climate and physical catchment structure. Hydrol. Earth Syst. Sci. 17, 1715–1732. https://doi.org/10.5194/hess-17-1715-2013.
Li, H., Sheffield, J., Wood, E.F., 2010. Bias correction of monthly precipitation and temperature fields from intergovernmental panel on climate change AR4 models using equidistant quantile matching. J. Geophys. Res. 115 (D10) https://doi.org/10.1029/2009JD012882.
Liu, M., Xu, X., Xu, C., Sun, A.Y., Wang, K., Scanlon, B.R., Zhang, L.u., 2017. A new drought index that considers the joint effects of climate and land surface change: a new drought index. Water Resour. Res. 53 (4), 3262–3278. https://doi.org/10.1002/2016WR020178.
Liu, S., Yan, D., Wang, H., Li, C., Weng, B., Qin, T., 2016. Standardized water budget index and validation in drought estimation of Haihe River Basin, North China. Adv. Meteorol. 2016, 1–10. https://doi.org/10.1155/2016/9159532.
Loh, W.-Y., 2011. Classification and regression trees. WIREs Data Mining Knowl. Discov. 1 (1), 14–23. https://doi.org/10.1002/widm.8.
Loon, A.F.V., Rangecroft, S., Coxon, G., Breña Naranjo, J.A., Ogtrop, F.V., Lanen, H.A.J.V., 2019. Using paired catchments to quantify the human influence on hydrological droughts. Hydrol. Earth Syst. Sci. 23, 1725–1739. https://doi.org/10.5194/hess-23-1725-2019.
López López, P., Sutanudjaja, E.H., Schellekens, J., Sterk, G., Bierkens, M.F.P., 2017. Calibration of a large-scale hydrological model using satellite-based soil moisture and evapotranspiration products. Hydrol. Earth Syst. Sci. 21, 3125–3144. https://doi.org/10.5194/hess-21-3125-2017.
Macqueen, J., 1967. Some methods for classification and analysis of multivariate observations, in: In 5-Th Berkeley Symposium on Mathematical Statistics and Probability. pp. 281–297.
Mallya, G., Mishra, V., Niyogi, D., Tripathi, S., Govindaraju, R.S., 2016. Trends and variability of droughts over the Indian monsoon region. Weath. Clim. Extrem. 12, 43–68. https://doi.org/10.1016/j.wace:2016.01.002.
Marcos-Garcia, P., Lopez-Nicolas, A., Pulido-Velazquez, M., 2017. Combined use of relative drought indices to analyze climate change impact on meteorological and hydrological droughts in a Mediterranean basin. J. Hydrol. 554, 292–305. https://doi.org/10.1016/j.jhydrol.2017.09.028.
Martens, B., Miralles, D.G., Lievens, H., van der Schalie, R., de Jeu, R.A.M., Fernández-Prieto, D., Beck, H.E., Dorigo, W.A., Verhoest, N.E.C., 2017. GLEAM v3: satellite-based land evaporation and root-zone soil moisture. Geosci. Model Dev. 10, 1903–1925. https://doi.org/10.5194/gmd-10-1903-2017.
McKee, T.B., Doesken NJ, Kleist J, 1993. The relationship of drought frequency and duration to time scales. In Proceedings of the 8th Conference on Applied Climatology. Boston, MA: American Meteorol Soci 17 (22), 179–183.
Miralles, D.G., Holmes, T.R.H., Jeu, R.A.M.D., Gash, J.H., Meesters, A.G.C.A., Dolman, A.J., 2011. Global land-surface evaporation estimated from satellite-based observations. Hydrol. Earth Syst. Sci. 15, 453–469. https://doi.org/10.5194/hess-15-453-2011.
Monish, N.T., Rehana, S., 2019. Suitability of distributions for standard precipitation and evapotranspiration index over meteorologically homogeneous zones of India. J. Earth Syst. Sci. 129 (1) https://doi.org/10.1007/s12040-019-1271-x.
Oloruntade, A.J., Mohammad, T.A., Ghazali, A.H., Wayayok, A., 2017. Analysis of meteorological and hydrological droughts in the Niger-South Basin, Nigeria. Global Planet. Change 155, 225–233. https://doi.org/10.1016/j.gloplacha.2017.05.002.
Pai, D.S., Sridhar, L., Rajeevan, M.C., Sreejith, O.P., Satbhai, N.S., Mukhopadhyay, B., 2014. Development of a new high spatial resolution ($0.25^\circ \times 0.25^\circ$) long period (1901-2010) daily gridded rainfall data set over India and its comparison with existing data sets over the region.
Rehana, S., 2019. River Water Temperature Modelling Under Climate Change Using Support Vector Regression, in: Singh, S.K., Dhanya, C.T. (Eds.), Hydrology in a Changing World: Challenges in Modeling, Springer Water. Springer International Publishing, Cham, pp. 171–183. https://doi.org/10.1007/978-3-030-02197-9_8.
Rehana, S., Monish, N.T., 2020. Characterization of Regional Drought Over Water and Energy Limited Zones of India Using Potential and Actual Evapotranspiration. Earth Space Sci. 7 (10) https://doi.org/10.1029/2020EA001264.
Rehana, S., Monish, N.T., Sireesha Naidu, G., 2020a. Estimation of annual regional drought index considering the joint effects of climate and water budget for Krishna River basin, India. Environ. Monit. Assess. 192 (7) https://doi.org/10.1007/s10661-020-08379-y.
Rehana, S., Mujumdar, P.P., 2012. Climate change induced risk in water quality control problems. J. Hydrol. 444-445, 63–77. https://doi.org/10.1016/j.jhydrol.2012.03.042.
Rehana, S., Naidu, G.S., Monish, N.T., 2020. Spatiotemporal Variations of Precipitation and Temperatures Under CORDEX Climate Change Projections: A Case Study of Krishna River Basin, India, in: Singh, P., Singh, R.P., Srivastava, V. (Eds.), Contemporary Environmental Issues and Challenges in Era of Climate Change. Springer, Singapore, pp. 157–170. https://doi.org/10.1007/978-981-32-9595-7_8.
Rehana, S., Sireesha Naidu, G., Monish, N.T., Sowjanya, U., 2020c. Modeling hydro-climatic changes of evapotranspiration over a semi-arid river basin of India. jwc2020173 J. Water Clim. Change. https://doi.org/10.2166/wcc.2020.173.
Rooijen, D.J.V., Turral, H., Biggs, T.W., 2009. Urban and industrial water use in the Krishna Basin, India. Irrig. Drain. 58, 406–428. https://doi.org/10.1002/ird.439.
Sajedi-Hosseini, F., Malekian, A., Choubin, B., Rahmati, O., Cipullo, S., Coulon, F., Pradhan, B., 2018. A novel machine learning-based approach for the risk assessment of nitrate groundwater contamination. Sci. Total Environ. 644, 954–962. https://doi.org/10.1016/j.scitotenv.2018.07.054.
Salvi, K., S., K., Ghosh, S., 2013. High-resolution multisite daily rainfall projections in India with statistical downscaling for climate change impacts assessment:

downscaling of Indian rainfall. J. Geophys. Res. Atmos. 118 (9), 3557–3578. https://doi.org/10.1002/jgrd.50280.
Shah, D., Mishra, V., 2020. Integrated drought index (IDI) for drought monitoring and assessment in India. Water Resour. Res. 56 (2) https://doi.org/10.1029/2019WR026284.
Shelton, M.L., 2008. Hydroclimatology: Perspectives and Applications [WWW Document]. Cambridge Core. https://doi.org/10.1017/CBO9780511754746.
Shukla, S., Wood, A.W., 2008. Use of a standardized runoff index for characterizing hydrologic drought. Geophys. Res. Lett. 35 (2) https://doi.org/10.1029/2007GL032487.
Sireesha Naidu, G., Pratik, M., Rehana, S., 2020. Modelling hydrological responses under climate change using machine learning algorithms – semi-arid river basin of peninsular India. H2Open Journal. https://doi.org/10.2166/h2oj.2020.034.
Srivastava, A.K., Rajeevan, M., Kshirsagar, S.R., 2009. Development of a high resolution daily gridded temperature data set (1969–2005) for the Indian region. Atmos. Sci. Lett. 10, 249–254. https://doi.org/10.1002/asl.232.
Thornthwaite, C.W., 1948. An approach toward a rational classification of climate. Geogr. Rev. 38 (1), 55. https://doi.org/10.2307/210739.
Tirivarombo, S., Osupile, D., Eliasson, P., 2018. Drought monitoring and analysis: standardised precipitation evapotranspiration index (SPEI) and standardised precipitation index (SPI). Phys. Chem. Earth, Parts A/B/C 106, 1–10. https://doi.org/10.1016/j.pce:2018.07.001.
Turc, L., 1954. The water balance of soils', relation between precipitation evaporation and flow. Ann. Agronom. 5, 491–569.
Vapnik, V., Golowich, S.E., Smola, A.J., 1997. Support Vector Method for Function Approximation, Regression Estimation and Signal Processing, in: Mozer, M.C., Jordan, M.I., Petsche, T. (Eds.), Advances in Neural Information Processing Systems 9. MIT Press, pp. 281–287.
Venot, J.P., B.R. Sharma, Rao, K.V.G.K., 2008. The lower Krishna Basin trajectory: relationships between basin development and downstream environmental degradation (No. IWMI Research Reports H041463, International Water Management Institute).
Vicente Serrano, S.M., Beguería, S., López-Moreno, J.I., 2010. A multi-scalar drought index sensitive to global warming: the standardized precipitation evapotranspiration index – SPEI. https://doi.org/10.1175/2009JCLI2909.1.
Wang, F., Wang, Z., Yang, H., Di, D., Zhao, Y., Liang, Q., 2020. A new copula-based standardized precipitation evapotranspiration streamflow index for drought monitoring. J. Hydrol. 585, 124793. https://doi.org/10.1016/j.jhydrol.2020.124793.
Waseem, M., Ajmal, M., Kim, T.-W., 2015. Development of a new composite drought index for multivariate drought assessment. J. Hydrol. 527, 30–37. https://doi.org/10.1016/j.jhydrol.2015.04.044.
Wilby, R.L., Dawson, C.W., 2013. The Statistical DownScaling Model: insights from one decade of application: SDSM-one decade on. Int. J. Climatol. 33 (7), 1707–1719. https://doi.org/10.1002/joc.3544.
Wilhite, D.A., Glantz, M.H., 1985. Understanding: the drought phenomenon: the role of definitions. Water Int. 10 (3), 111–120. https://doi.org/10.1080/02508068508686328.
Wu, J., Miao, C., Wang, Y., Duan, Q., Zhang, X., 2017. Contribution analysis of the long-term changes in seasonal runoff on the Loess Plateau, China, using eight Budyko-based methods. J. Hydrol. 545, 263–275. https://doi.org/10.1016/j.jhydrol.2016.12.050.
Yang, D., Sun, F., Liu, Z., Cong, Z., Ni, G., Lei, Z., 2007. Analyzing spatial and temporal variability of annual water-energy balance in nonhumid regions of China using the Budyko hypothesis: variability in annual water balance. Water Resour. Res. 43 (4) https://doi.org/10.1029/2006WR005224.
Yang, X., Yong, B., Ren, L., Zhang, Y., Long, D.i., 2017a. Multi-scale validation of GLEAM evapotranspiration products over China via ChinaFLUX ET measurements. Int. J. Remote Sens. 38 (20), 5688–5709. https://doi.org/10.1080/01431161.2017.1346400.
Yang, Y., McVicar, T.R., Donohue, R.J., Zhang, Y., Roderick, M.L., Chiew, F.H.S., Zhang, L.u., Zhang, J., 2017b. Lags in hydrologic recovery following an extreme drought: assessing the roles of climate and catchment characteristics. Water Resour. Res. 53 (6), 4821–4837. https://doi.org/10.1002/2017WR020683.
YUE, SHENG, HASHINO, MICHIO, 2007. Probability distribution of annual, seasonal and monthly precipitation in Japan. Hydrol. Sci. J. 52 (5), 863–877. https://doi.org/10.1623/hysj.52.5.863.
Zhang, K.e., Kimball, J.S., Nemani, R.R., Running, S.W., 2010. A continuous satellite-derived global record of land surface evapotranspiration from 1983 to 2006: global record of land surface evapotranspiration. Water Resour. Res. 46 (9) https://doi.org/10.1029/2009WR008800.
Zhang, L., Hickel, K., Dawes, W.R., Chiew, F.H.S., Western, A.W., Briggs, P.R., 2004. A rational function approach for estimating mean annual evapotranspiration: estimating mean annual evapotranspiration. Water Resour. Res. 40 (2) https://doi.org/10.1029/2003WR002710.